J. Phys. Chem. A **2009,** *113,* 7861–7877

Accurate Thermochemistry for Transition Metal Oxide Clusters

Shenggang Li, Jamie M. Hennigan, and David A. Dixon*

Chemistry Department, The University of Alabama, Shelby Hall, Box 870336,
Tuscaloosa, Alabama 35487-0336

Kirk A. Peterson

Department of Chemistry, Washington State University, Pullman, Washington 99164-4630

Received: November 19, 2008; Revised Manuscript Received: April 21, 2009

Total atomization energies (TAEs) and normalized clustering energies (NCEs) of group IVB $(MO_2)_n$ (M = Ti, Zr, Hf) and VIB $(MO_3)_n$ (M = Cr, Mo, W) transition metal oxide clusters up to $n = 4$ were calculated at the coupled cluster [CCSD(T)] and density functional theory (DFT) levels. For all the clusters studied, the TAEs calculated at the CCSD(T) level were found to be strongly basis set dependent, whereas the NCEs were significantly less basis set dependent. Here we further develop an efficient strategy for calculating accurate thermodynamic properties of large clusters based on those of the cluster unit and the NCEs. The calculated TAEs, NCEs, and heats of formations for these clusters were compared with available experimental data. We also benchmarked the performance of popular DFT exchange−correlation functionals for the calculations of the TAEs and NCEs. The performance of many DFT functionals for the calculation of the TAEs strongly depends on the choice of the electronic state for the transition metal atom. Hybrid functionals were found to generally outperform pure functionals in the calculation of NCEs, and the PBE1PBE functional has the best performance with average deviations of ∼1 kcal/mol for the dimers and ∼2 kcal/mol for the trimers and tetramers. The benchmarked functionals all display gradual degradation in performance with increasing cluster size.

Introduction

Transition metal oxides (TMOs) form an important class of materials widely employed in industry as heterogeneous catalysts or catalyst supports. Unlike oxides of main group metal elements, TMOs can serve as both acid−base and redox catalysts.[1] Examples of the redox reactions catalyzed by TMOs are the synthesis gas reaction as an important step for the efficient transformation of natural gas, the reduction of NO_x in automotive exhaust for environmental protection, and the selective oxidation of alkanes, alkenes, and alcohols for the chemical industry.[2] Over the past few decades, photocatalysts based on TMOs, notably TiO_2, have received significant interest due to the potential for the efficient utilization of solar energy, and more recently for environmental clearance.[3] In addition, there is significant interest in metal oxides for use in the semiconductor industry as high dielectric materials.

TMO clusters are often used as models for catalysts, and in some cases, as actual catalysts, for example, the polyoxometalates.[4] The accurate prediction of cluster structures and reaction energetics are critical to the successful modeling of the behavior of TMO catalysts. An important thermodynamic property needed for any reaction is the heat of formation of a species. Although heats of formation for compounds of main group elements can now be somewhat routinely predicted with high accuracy, for example, with composite methods (the Gaussian-*N* methods,[5] the Weizmann-*N* methods,[6] the complete basis set (CBS) methods,[7] the CBS approaches developed at the Pacific Northwest National Laboratory and Washington State University,[8] and the HEAT method[9]), such approaches have not been widely used for transition metal compounds. One of the reasons is that these methods were developed for compounds of main group elements. This is evident from the test set for the Gaussian-*N* methods[10] and the latest G4 method,[5d] which are based on energetics of compounds involving the first three main row group elements. The exclusion of the compounds of the heavier main group elements and especially those of the transition elements is partially due to the lack of accurate experimental data. Very recently, the correlation consistent composite approach (ccCA)[11] has been benchmarked for the calculation of heats of formation for a set of first row transition metal compounds.[12] The CBS approach based on the coupled cluster method[8] and the ccCA approach were found to have mean absolute deviations of 3.1 and 3.4 kcal/mol, respectively, which are close to the initial goal of “chemical accuracy” of ±3 kcal/mol for transition metal model chemistries defined by the ccCA group.

Coupled cluster methods, especially CCSD(T), have emerged as one of the most accurate and yet generally applicable methods in quantum chemistry.[13] In addition, the development of the correlation consistent basis sets, which allows for the extrapolation of the electronic energy to the CBS limit, has proven critical for reaching chemical accuracy in the calculated energetics.[14] The recent design of systematically convergent, correlation consistent basis sets for the third, fourth, and fifth row main group and transition elements using relativistic effective core potentials (RECPs)[15] has been essential to the application of highly accurate correlation methods to most of the elements in the periodic table. For relatively large systems, the CCSD(T) method is still impractical, and density functional theory (DFT)[16]

---

* Corresponding author. E-mail: dadixon@bama.ua.edu.

10.1021/jp810182a CCC: $40.75

is the most computationally efficient method that can potentially achieve reasonable accuracy at the present.

We have recently carried out accurate calculations on group IVB and VIB TMO clusters, where we predicted cluster structures, electron detachment energies, clustering energies, and heats of formation and compared the with available experimental data.[17,18] We have shown that the CCSD(T) method together with the recently developed correlation consistent basis sets based on RECPs is capable of providing accurate electron detachment energies and heats of formation for these clusters. For DFT, we have found that the BP86[19,20] and PW91[21,22] exchange−correlation functionals provide excellent electron detachment energies but fail to provide accurate heats of formation.[17b] In addition, our recent studies on the $(TiO_2)_n$ ($n = 1-4$) clusters have shown that the total atomization energies (TAEs) and thus the heats of formation for these clusters calculated from them at the CCSD(T) level are strongly basis set dependent, whereas the clustering energies are much less basis set dependent.[17d] We thus developed a computationally efficient approach to calculate accurate heats of formation for the large clusters based on the calculated clustering energies.

The purpose of the current work is 3-fold: (1) to provide accurate heats of formation for the group IVB and VIB TMO clusters; (2) to further develop and apply an effective and accurate approach for calculating the heats of formation for the larger clusters from the normalized clustering energies (NCEs); and (3) to benchmark the performance of common DFT exchange−correlation functionals for the accurate calculation of the TAEs and NCEs. DFT benchmarks for transition metal compounds have recently been carried out by Truhlar and co-workers predominantly for transition metal diatomics and a few transition metal complexes with a range of functionals,[23,24] and by Furche and Perdew on first row transition metal diatomics for six functionals,[25] for example. We have chosen a representative set of 27 exchange−correlation functionals for our benchmarks, as in our recent benchmarks of electron detachment energies[17b,c] and adiabatic ionization potentials.[26] These potentials were chosen because they cover pure generalized gradient approximation potentials (GGAs) of practical use in plane wave calculations as well commonly used hybrid functionals. The approach we have developed for the accurate calculations of the heats of formation of the large clusters here is related to the isodesmic reaction approach,[27] and thus it should be generally applicable to other transition metal compounds than these TMO clusters.

Computational Methods. Geometries were optimized and harmonic frequencies were calculated at the DFT level with the B3LYP[28,29] and BP86 exchange−correlation functionals for the ground states of the $(MO_2)_n$ and $(M'O_3)_n$ (M = Ti, Zr, Hf; M′ = Cr, Mo, W; $n = 1-4$) clusters. Single point energy calculations were carried out with a wide variety of currently available exchange−correlation functionals at the B3LYP geometries. These functionals are (1) local spin density approximation (LSDA) SVWN5;[30,31] (2) generalized gradient approximations (GGAs) BLYP,[19,29] BP86, BPW91,[19,22] BB95,[19,32] PW91, mPWPW91,[33,22] PBE,[34,35] OLYP,[36,29] TPSS,[37] and VSXC[38] and the Handy family of functionals HCTH93, HCTH147, HCTH407;[39] and (3) hybrid GGAs B3LYP, B3P86, B3PW91,[28] B1B95,[32] B1LYP, mPW1PW91,[40] B98,[41] B971,[42] B972,[43] PBE1PBE,[34] O3LYP,[44] TPSSh,[37] and BMK.[45]

We use the augmented correlation consistent aug-cc-pVnZ basis set for O[14b] and the aug-cc-pVnZ-PP relativistic effective core potential (RECP) basis sets for the transition metal atoms[15d] in the DFT optimization and frequency calculations with n = D and in the DFT single point energy calculations with n = T; these basis sets are collectively denoted as aVDZ-PP and aVTZ-PP. Although the DFT method is much less basis set dependent than the wave function-based methods, for the monomer and dimer we have also calculated the single point energies at the B3LYP level with the aVQZ-PP basis set (n = Q). For these molecules, we extrapolated the B3LYP energies to the complete basis set (CBS) limit using a mixed Gaussian/exponential formula[46]

$$E(n) = E_{CBS} + A\exp[-(n-1)] + B\exp[-(n-1)^2] \qquad (1)$$

with $n = 2$, 3, and 4 for the aVDZ-PP, aVTZ-PP, and aVQZ-PP basis sets, respectively. A similar exponential extrapolation has been found to work well for Hartree−Fock energies as well as eq 1, hence our choice of eq 1 for the DFT extrapolations with this range of basis sets. Wilson and co-workers[47] who tested a number of extrapolation schemes have found that an exponential function (eq 2) originally suggested by Feller[48]

$$E(n) = E_{CBS} + A^*\exp(-Bx) \qquad (2)$$

works slightly better than eq 1 for extrapolating the Hartree−Fock energies for small transition metal molecules when compared to numerical HF results. We also used this expression and found that the total energies for the atoms differed by 0.08, 0.04, 0.05, 0.13, 0.03, and 0.02 kcal/mol for Ti, Zr, Hf, Cr, Mo, and W, respectively. The O atom extrapolation differed by 0.47 kcal/mol, and thus this dominates the molecular clusters. The extrapolation in the atomization energies differed by −1.35 kcal/mol for W_2O_6 to 0.43 kcal/mol for CrO_3. The differences in the energy extrapolations are given as Supporting Information.

For the monomer and dimer, CCSD(T) calculations were performed with the sequence of basis sets aug-cc-pVnZ for O[14b] and aug-cc-pVnZ-PP for the metal atoms[15d] with n = D, T, Q with the geometries optimized at the CCSD(T) levels for n = D and T. The CCSD(T) total energies were extrapolated to the CBS limit using eq 1. Our recent studies on the group VIB transition metal oxide clusters have shown that the effect of the choice of the value of n in this extrapolation scheme is fairly small.[17b]

Core−valence correlation corrections were calculated at the CCSD(T) level with the aug-cc-pwCVnZ basis set for O[49,50] and the aug-cc-pwCV*n*Z-PP basis set for the transition metal atoms,[15d] with n = D and T. These basis sets will be collectively denoted as awCVDZ-PP and awCVTZ-PP respectively. The core−valence corrections were also calculated without the extra diffuse functions, and these basis sets are denoted as wCVDZ-PP and wCVTZ-PP, respectively. In addition, scalar relativistic corrections for the O atoms were calculated as expectation values of the mass-velocity and Darwin (MVD) operators at the CISD (configuration interaction with single and double excitations) and HF (Hartree−Fock) levels with the aVTZ-PP basis set. A potential problem arises in computing this scalar relativistic correction for the molecules in this study, as there is the possibility of "double counting" the relativistic effect on the metal when applying a MVD correction to an energy that already includes most relativistic effects via the RECP. Because the MVD operators mainly sample the core region where the pseudo-orbitals are small, we assume any double counting to be small as has been found for halogen thermodynamics.[51]

To estimate the errors for using the RECP basis sets in the above procedure, CCSD(T) calculations were also performed at the second order Douglas−Kroll−Hess (DK) level with the all-electron DK basis sets. For M = Ti and Cr, the CCSD(T)-DK calculations were carried out with the aug-cc-pVnZ-DK basis sets for O,[52] Ti, and Cr[53] with n = D, T, and Q; these basis sets will be collectively denoted as aVnZ-DK. For M = Zr, Mo, Hf, and W, the CCSD(T)-DK calculations were performed with the aVTZ-DK basis set,[15d] which is the only correlation-consistent DK basis set available. Core−valence corrections were also calculated at the CCSD(T)-DK level with the aug-cc-pwCVTZ-DK and cc-pwCVTZ-DK basis sets;[15d,50,53] these basis sets will be collectively denoted as awCVTZ-DK and wCVTZ-DK. For M = Hf and W, additional high angular momentum functions (2f2g1h)[15d] for correlating the metal 4f orbitals in the core−valence calculations were included as these orbitals are higher in energy than the metal 5s and 5p orbitals. The valence electronic energy calculated at the CCSD(T)-DK/awCVTZ-DK level ($\Delta E_{\text{awCVTZ-DK}}$) were used to correct the error in the valence electronic energy calculated at the CCSD(T) level with the RECP basis sets, $\Delta E_{\text{PP,corr}}$,

$$\Delta E_{\text{PP,corr}} = \Delta E_{\text{awCVTZ-DK}} - (\Delta E_{\text{awCVTZ-PP}} + \Delta E_{\text{SR}}) \tag{3}$$

where $\Delta E_{\text{awCVTZ-PP}}$ is the valence electronic energy calculated at the CCSD(T)/awCVTZ-PP level and ΔE_{SR} is the scalar relativistic correction calculated as the MVD expectation values. This correction factor was then used to correct the valence electronic energy calculated at the CCSD(T)/CBS level with the RECP basis sets [ΔE_{CBS} (PP)] to give the corrected valence CBS energy [$\Delta E_{\text{Val,corr}}$ (PP)] with the scalar relativistic correction (ΔE_{SR}) as

$$\begin{aligned}\Delta E_{\text{Val,corr}}(\text{PP}) &= \Delta E_{\text{CBS}}(\text{PP}) + \Delta E_{\text{SR}} + \Delta E_{\text{PP,corr}}\\ &= \Delta E_{\text{CBS}}(\text{PP}) + \Delta E_{\text{awCVTZ-DK}} - \Delta E_{\text{awCVTZ-PP}}\end{aligned} \tag{4}$$

In eq 4, the scalar relativistic correction for the O atoms comes from the $\Delta E_{\text{awCVTZ-DK}}$ term due to cancellation of the ΔE_{SR} term. In addition, for HfO_2 and WO_3, we also carried out the CCSD(T) calculations at the DK level to third order (DK3) with the aug-cc-pVTZ-DK3 and aug-cc-pwCVTZ-DK3 basis sets,[15d] and the total atomization energies calculated at the DK3 level are larger than those calculated at the DK level to second order by 0.2 to 0.3 kcal/mol.

For the trimer and tetramer, the CCSD(T) calculations were performed with the aVDZ-PP and aVTZ-PP basis sets at the B3LYP/aVDZ-PP geometries. The B3LYP/aVDZ-PP geometries were used for these CCSD(T) calculations as the B3LYP/aVTZ-PP geometries calculated for the monomers given as Supporting Information are no better than the B3LYP/aVDZ-PP geometries when compared with the CCSD(T)/aVTZ-PP geometries. Core−valence corrections were calculated at the CCSD(T) level with the wCVDZ-PP, awCVDZ-PP, and wCVTZ-PP basis sets, and scalar relativistic corrections were calculated as MVD expectation values of the CISD/aVTZ-PP and HF/aVTZ-PP wave functions. Similar calculations at the CCSD(T)-DK level were carried out with the all-electron DK basis sets for these clusters.

All DFT calculations were performed with the Gaussian 03 program package.[54] For the pure DFT methods, the density fitting approximation was employed to speed up the calculations.[55] The density fitting sets were automatically generated from the atomic orbital primitives.[54] The CCSD(T) calculations were performed with the MOLPRO 2006.1[56] and NWChem 5.1[57] program packages. The calculations were performed on the Opteron-based Cray XD1, Dense Memory Cluster (DMC), and Itanium 2-based SGI Altix supercomputers at the Alabama Supercomputer Center, the Xeon-based Dell Linux cluster at the University of Alabama, the local Opteron-based Parallel Quantum Solutions Linux cluster, and the Itanium 2-based Linux cluster at the Molecular Science Computing Facility from the Pacific Northwest National Laboratory.

Following our previous work,[17a,d] the normalized clustering energy (NCE) of $(MO_m)_n$, $\Delta E_{\text{norm},n}$, is defined as

$$\Delta E_{\text{norm},n} = \{nE(\text{MO}_m) - E[(\text{MO}_m)_n]\}/n \tag{5}$$

The NCE is the average binding energy of the monomers in a cluster.

The total atomization energy (TAE) of $(MO_m)_n$ at 0 K for $n = 1$ and 2 is calculated as the energy difference between the ground states of the atoms and that of the cluster,[17b,d]

$$\sum D_{0,0\text{K}} = nE(\text{M}) + m{*}nE(\text{O}) - E[(\text{MO}_m)_n] \tag{6}$$

At the CCSD(T) level, the TAE is calculated as the sum of various contributions,

$$\begin{aligned}\sum D_{0,0\text{K}} &= \Delta E_{\text{CBS}} + \Delta E_{\text{SR}} + \Delta E_{\text{PP,corr}} + \Delta E_{\text{CV}} + \\ &\qquad \Delta E_{\text{ZPE}} + \Delta E_{\text{SO}}\\ &= \Delta E_{\text{CBS}} + \Delta E_{\text{awCVTZ-DK}} - \Delta E_{\text{awCVTZ-PP}} + \\ &\qquad \Delta E_{\text{CV}} + \Delta E_{\text{ZPE}} + \Delta E_{\text{SO}}\end{aligned} \tag{7}$$

The spin−orbit contributions (ΔE_{SO}) are calculated from the experimental values for the ground states of the atoms.[58] For M = W, we calculated the atomization energy relative to the first excited state of the atom ($^7S_3$) and corrected the calculated TAE with the experimental energy difference of 8.44 kcal/mol between this state and the $^5D_0$ ground state. At the CCSD(T)-DK level, eq 7 reduces to

$$\sum D_{0,0\text{K}} = \Delta E_{\text{CBS}} + \Delta E_{\text{CV}} + \Delta E_{\text{ZPE}} + \Delta E_{\text{SO}} \tag{8}$$

At the DFT level, eq 7 further reduces to

$$\sum D_{0,0\text{K}} = \Delta E_{\text{CBS}} + \Delta E_{\text{ZPE}} + \Delta E_{\text{SO}} \tag{9}$$

The heat of formation of $(MO_m)_n$ at 0 K for $n = 1$ and 2 is calculated from its TAE and the experimental heats of formation of the atoms[59]

$$\begin{aligned}\Delta H_{\text{f,0K}}[(\text{MO}_m)_n] = n\Delta H_{\text{f,0K}}(\text{M}) + m{*}n\Delta H_{\text{f,0K}}(\text{O}) - \\ \sum D_{0,0\text{K}}[(\text{MO}_m)_n]\end{aligned} \tag{10}$$

Heats of formation at 298 K are calculated by following the procedures outlined by Curtiss et al.[60] For $n = 3$ and 4, the heat of formation of $(MO_m)_n$ at 0 K is calculated from its NCE

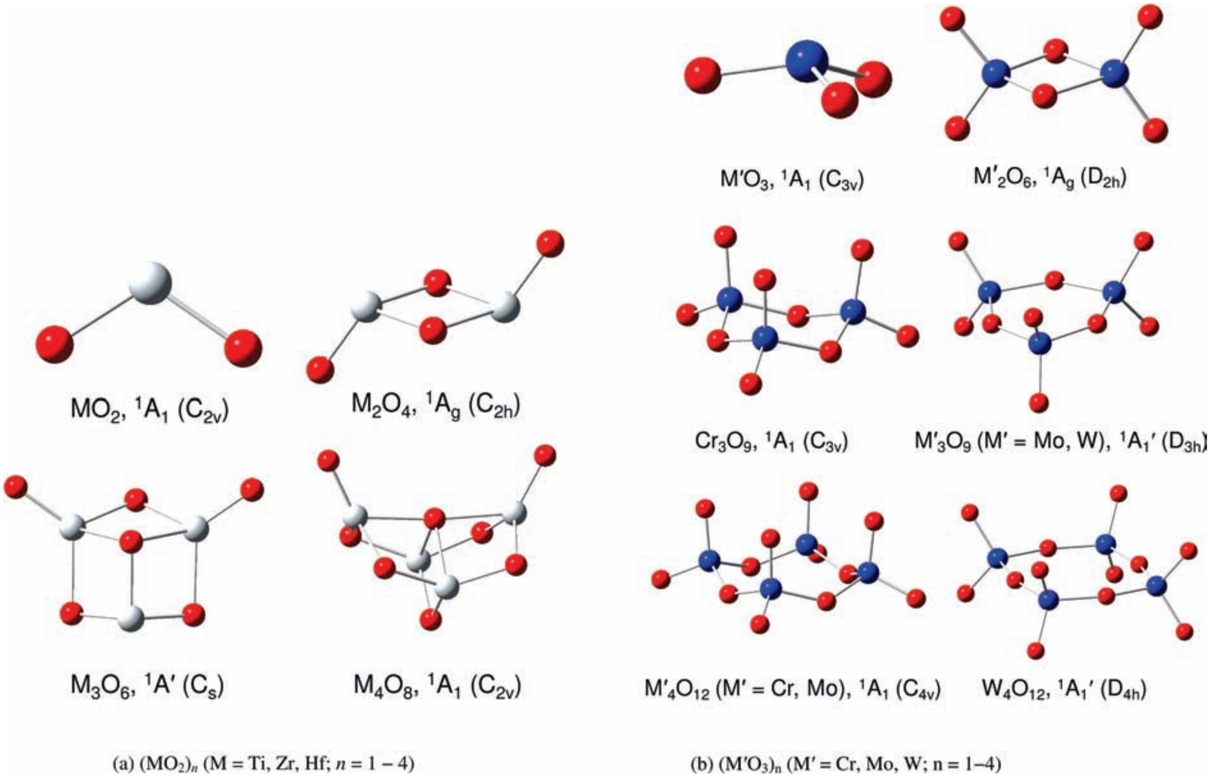

(a) $(MO_2)_n$ (M = Ti, Zr, Hf; n = 1 – 4)

(b) $(M'O_3)_n$ (M′ = Cr, Mo, W; n = 1–4)

Figure 1. Ground state structures of the $(MO_2)_n$ and $(M'O_3)_n$ (M = Ti, Zr, Hf; M′ = Cr, Mo, W; n = 1−4) clusters.

and the calculated heat of formation of the monomer following our previous work[17d]

$$\Delta H_{\mathrm{f,0K}}[(\mathrm{MO}_m)_n] = n\Delta H_{\mathrm{f,0K}}(\mathrm{MO}_m) - n\Delta E_{\mathrm{norm},n}[(\mathrm{MO}_m)_n] \tag{11}$$

For $n = 2$, the above two approaches for calculating the heats of formation yield identical results for this study.

Results and Discussion

Figure 1 shows the ground state structures of the $(MO_2)_n$ and $(M'O_3)_n$ (M = Ti, Zr, Hf; M′ = Cr, Mo, W; n = 1−4) clusters. They have been discussed elsewhere.[17,18] For M = Cr, Mo, and W, no low-lying isomers have been predicted for the monomer and dimer. For the trimer and tetramer, the chain isomer was calculated to be 25−50 kcal/mol higher in energy than the ground state ring isomer at the B3LYP level with a triple-ζ basis set.[17a] For M = Ti, Zr, and Hf, no low-lying isomer was predicted for the monomer. For the larger clusters where low-lying isomers are present, the lowest energy isomer was predicted to be more than 3 kcal/mol higher in energy at the CCSD(T) level at the complete basis set limit for the dimer and with a triple-ζ basis set for the trimer and tetramer.[17d,18]

Total Atomization Energies of Monomers and Dimers. The total atomization energies (TAEs) at 0 K for the monomers and dimers were calculated as sums of the valence electronic energy with the scalar relativistic and pseudopotential corrections (Tables 1 and Tables 2), and the core−valence, zero-point energy (ZPE), and spin−orbit corrections (Table 3).

Table 1 presents the valence electronic energy contributions to the TAEs calculated at the CCSD(T) level with the RECP basis sets and at the CCSD(T)-DK level with the all-electron DK basis sets for M = Ti and Cr. Those calculated with the RECP basis sets were corrected with the pseudopotential corrections. Those calculated at the CCSD(T) level with the RECP basis sets and corrected with the pseudopential corrections for the other metals are given in Table 2. The calculated pseudopotential corrections ($\Delta E_{\mathrm{PP,corr}}$) from eq 3 are to increase the TAEs by ~0.2 kcal/mol for TiO_2, by 0.7−1.0 kcal/mol for CrO_3 and Ti_2O_4, and by ~2.2 kcal/mol for Cr_2O_6. These can be compared to the analogous values for the atoms for their ionization potentials and low-lying excitation energies of 0.2−0.4 kcal/mol.[15d] In comparison with the valence electronic energy contributions to the TAEs calculated at the CCSD(T)-DK level, those calculated at the CCSD(T) level with the scalar relativistic and pseudopotential corrections are larger by ~0.1 kcal/mol for TiO_2, by 0.4−0.5 kcal/mol for CrO_3 and Ti_2O_4, and by ~0.9 kcal/mol for Cr_2O_6 ($\Delta\Delta E_{\mathrm{Val}}$). These latter differences, however, do not necessarily reflect a large basis set dependence in the pseudopotential correction, but mostly an uncertainty in the CBS extrapolations for the PP energies as compared to the DK energies. As expected from our previous work,[51] the potential for double counting in the use of the MVD correction with the RECP is small. In particular, the cc-pVDZ-DK basis set is significantly different from cc-pVDZ-PP, since the former was derived using a triple-ζ Hartree−Fock basis set and an atomic natural orbital (ANO) expansion for the d-type correlating function.[53b] Hence it should have considerably less basis set superposition error (BSSE) compared to cc-pVDZ-PP and will yield slightly different CBS limits in the present extrapolation scheme. This is easily observed by comparing the TAEs of Cr_2O_6 calculated at the CCSD(T)/aVnZ-PP and CCSD(T)/aVnZ-DK levels (n = D, T) as shown in Table 1.

The pseudopotential corrections for ZrO_2 and Zr_2O_4 (Table 2) are to increase the TAEs by ~0.5 and 1.2 kcal/mol, respectively, and those for MoO_3 and Mo_2O_6 are to increase the TAEs by ~2.9 and 6.2 kcal/mol. For WO_3 and W_2O_6, the pseudopotential corrections are to reduce the TAEs by ~1.2

TABLE 1: Valence Electronic Energy Contributions to the Total Atomization Energies in kcal/mol for the Ground States of $(TiO_2)_n$ and $(CrO_3)_n$ (n = 1−2) Calculated at the CCSD(T) Level with the Pseudopotential Corrections and at the CCSD(T)-DK Level[a]

	molecule							
	TiO_2		Ti_2O_4		CrO_3		Cr_2O_6	
	PP	DK	PP	DK	PP	DK	PP	DK
$\Delta E_{n=D}$[b]	280.73	277.76	682.83	676.42	314.34	307.92	719.96	709.61
$\Delta E_{n=T}$[c]	291.55	290.97	704.79	703.53	330.69	329.26	754.88	751.94
$\Delta E_{n=Q}$[c]	296.67	296.08	715.26	713.91	337.61	336.03	768.59	765.35
ΔE_{CBS}[d]	299.77	299.08	721.59	719.98	341.72	339.87	776.65	772.96
ΔE_{SR}[c,e]	−0.78		−2.19		−2.09		−5.03	
ΔE_{Val}[f]	298.99	299.08	719.40	719.98	339.63	339.87	771.62	772.96
ΔE_{awCVTZ}[c,g]	292.65	292.09	706.43	705.23	331.32	329.96	755.61	752.82
$\Delta E_{PP,corr}$[h]	+0.22		+0.99		+0.73		+2.24	
$\Delta E_{Val,corr}$[i]	299.21		720.39		340.36		773.86	
$\Delta\Delta E_{Val}$[j]	+0.13		+0.41		+0.49		+0.90	

[a] Each term was calculated from eq 6 as the energy difference between the ground states of the atoms ($^3F_2$ for Ti, $^7S_3$ for Cr, and $^3P_2$ for O) and the cluster. [b] Geometries from CCSD(T)/aVDZ-PP. [c] Geometries from CCSD(T)/aVTZ-PP. [d] Extrapolated CCSD(T) or CCSD(T)-DK energies with n = D, T, and Q using eq 1. [e] MVD Expectation values of the CISD/aVTZ-PP wave function. [f] $\Delta E_{Val}(PP) = \Delta E_{CBS}(PP) + \Delta E_{SR}$, and $\Delta E_{Val}(DK) = \Delta E_{CBS}(DK)$. [g] Valence electronic energies at the CCSD(T)/awCVTZ-PP and CCSD(T)-DK/awCVTZ-DK levels. [h] Equation 3: $\Delta E_{PP,corr} = \Delta E_{awCVTZ\text{-}DK} - (\Delta E_{awCVTZ\text{-}PP} + \Delta E_{SR})$. [i] Equation 4: $\Delta E_{Val,corr}(PP) = \Delta E_{Val}(PP) + \Delta E_{PP,corr} = \Delta E_{CBS}(PP) + \Delta E_{awCVTZ\text{-}DK} - \Delta E_{awCVTZ\text{-}PP}$. [j] $\Delta\Delta E_{Val} = \Delta E_{Val,corr}(PP) - \Delta E_{Val}(DK)$.

TABLE 2: Valence Electronic Energy Contributions to the Total Atomization Energies in kcal/mol for the Ground States of $(MO_2)_n$ and $(M'O_3)_n$ (M = Zr, Hf; M′ = Mo, W; n = 1−2) Calculated at the CCSD(T) Level with the Pseudopotential Corrections[a]

molecule	$\Delta E_{n=D}$[b]	$\Delta E_{n=T}$[c]	$\Delta E_{n=Q}$[c]	ΔE_{CBS}[d]	ΔE_{SR}[c,e]	ΔE_{Val}[f]	$\Delta E_{awCVTZ\text{-}PP}$[c,g]	$\Delta E_{awCVTZ\text{-}DK}$[c,h]	$\Delta E_{PP,corr}$[i]	$\Delta E_{Val,corr}$[j]
ZrO_2	306.91	322.15	327.76	331.02	−0.43	330.59	324.37	324.40	+0.46	331.05
HfO_2	305.31	321.07	326.77	330.08	−0.44	329.64	323.83	318.91	−4.48	325.16
MoO_3	378.85	404.01	412.48	417.33	−0.63	416.70	406.28	408.54	+2.89	419.59
WO_3	435.53	462.33	470.88	475.74	−0.61	475.13	464.48	462.72	−1.15	473.98
Zr_2O_4	743.23	772.50	783.91	790.61	−1.10	789.51	776.02	776.10	+1.18	790.69
Hf_2O_4	760.69	791.58	803.24	810.06	−1.10	808.96	798.73	788.00	−9.63	799.33
Mo_2O_6	868.43	920.28	937.19	946.83	−1.57	945.26	924.04	928.63	+6.16	951.42
W_2O_6	997.73	1053.30	1070.57	1080.33	−1.51	1078.82	1056.78	1053.11	−2.16	1076.66

[a] Each term was calculated from eq 6 as the energy difference between the ground states of the atoms ($^3F_2$ for Zr, Hf, $^7S_3$ for Mo, and $^3P_2$ for O) and the cluster. For W, the first excited state ($^7S_3$) was used, and the total atomization energy was corrected by its excitation energy from the ground state ($^5D_0$) of 8.44 kcal/mol. [b] Geometries from CCSD(T)/aVDZ-PP. [c] Geometries from CCSD(T)/aVTZ-PP. [d] Extrapolated CCSD(T) energies with n = D, T, and Q using eq 1. [e] MVD Expectation values of the CISD/aVTZ-PP wave function. [f] $\Delta E_{Val}(PP) = \Delta E_{CBS}(PP) + \Delta E_{SR}$. [g] Valence electronic energies at the CCSD(T)/awCVTZ-PP level. For M = Hf, the metal $5s^25p^6$ and oxygen $1s^2$ electrons were also correlated. [h] Valence electronic energies at the CCSD(T)-DK/awCVTZ-DK level. For M = Hf, the metal $5s^25p^{66}4f^{14}$ and oxygen $1s^2$ electrons were also correlated. [i] Equation 3: $\Delta E_{PP,corr} = \Delta E_{awCVTZ\text{-}DK} - (\Delta E_{awCVTZ\text{-}PP} + \Delta E_{SR})$. [j] Equation 4: $\Delta E_{Val,corr}(PP) = \Delta E_{Val}(PP) + \Delta E_{PP,corr} = \Delta E_{CBS}(PP) + \Delta E_{awCVTZ\text{-}DK} - \Delta E_{awCVTZ\text{-}PP}$.

and 2.2 kcal/mol, respectively, whereas for HfO_2 and Hf_2O_4, they are to reduce the TAEs by ~4.5 and 9.6 kcal/mol.

Very recently, DeYonker et al. calculated the TAEs of a number of transition metal compounds including CrO_3 by extrapolating the CCSD(T)-DK/aVnZ-DK (n = Q, 5) energies and including the other corrections.[12] For CrO_3, they have obtained a CBS value of 341.6 kcal/mol using the inverse cubic formula

$$E(l_{max}) = E_{CBS} + B/l_{max}^{\;3} \qquad (12)$$

for the correlation energy with an l_{max} equal to n for main group elements and their compounds and equal to $n + {}^1/_2$ for transition metal elements and their compounds and an exponential fit for the Hartree−Fock (HF) component. This CBS value is to be compared with our values of 339.9 and 340.1 kcal/mol obtained by extrapolating the CCSD(T)-DK/aVnZ-DK (n = D, T, Q) total energies and the CCSD(T)-DK/aVnZ-DK (n = T, Q, 5) total energies with eq 1, and 342.9 kcal/mol by extrapolating the CCSD(T)-DK/aVnZ-DK (n = Q, 5) correlation energies with eq 12 and with l_{max} equal to n for main group elements and $n + {}^1/_2$ for transition metal elements and their oxides and an exponential fit for the HF energies.

Previously,[17b] we found that the CBS energies obtained with eq 12 for transition metal compounds with n = Q and 5 depend strongly on the choice of l_{max} compared to those with eq 1. We obtained CBS values of 342.8, 344.5, and 346.2 kcal/mol with the value of l_{max} chosen as n, $n + {}^1/_2$, and $n + 1$ for transition metals and their compounds by extrapolating the n = Q and 5 correlation energies with eq 12 and with an exponential fit for the HF energies. We found similar behavior for the CCSD(T)-DK extrapolated energies. The extrapolated values using *total energies* and eq 12 for n = Q and 5 are 341.2, 342.9, and 344.6 kcal/mol with l_{max} chosen as n, $n + {}^1/_2$, and $n + 1$, whereas that using eq 1 for n = T, Q, 5 is 340.1 kcal/mol for n, $n + {}^1/_2$, and $n + 1$. The extrapolated values using eq 1 for n = D, T, Q are 339.9, 340.3, and 340.5 kcal/mol with n, $n + {}^1/_2$, and $n + 1$. As we have found previously,[12,17b] energy extrapolation with eq 12 is sensitive to the choice of l_{max} and tends to overestimate the CBS energy. On the other hand, extrapolation with eq 1 tends to underestimate the CBS energy but is less dependent on the choice of n. We have chosen to use eq 1 for the extrapolation in this work, which could introduce an error of a

TABLE 3: Total Atomization Energies at 0 K ($\Sigma D_{0,0K}$, kcal/mol) and Heats of Formation at 0 and 298 K for the Ground States of $(MO_2)_n$ and $(M'O_3)_n$ (M = Ti, Zr, Hf; M′ = Cr, Mo, W; n = 1−2) Calculated at the CCSD(T)-DK Level for M = Ti and Cr and at the CCSD(T) Level with the Pseudopotential Corrections for M = Zr, Hf, Mo, and W, and Compared with Available Experimental Data

molecule	ΔE_{Val}[a]	ΔE_{CV}[b]	ΔE_{ZPE}[c]	ΔE_{SO}[d]	$\Sigma D_{0,0K}$[e]	$\Delta H_{f,0K}$[f]	$\Delta H_{f,298K}$[g]	expt (298K)[h]
TiO_2	299.08	+2.93	−3.26	−1.08	297.67	−67.3	−67.9	−73.0 ± 3 −71.4 ± 3[i]
ZrO_2	331.05	+2.89	−2.91	−2.51	328.52	−66.7	−67.4	−68.4 ± 11
HfO_2	325.16	+0.80	−2.83	−8.29	314.84	−49.2	−50.0	
CrO_3	339.87	−0.64	−5.77	−0.67	332.79	−61.4	−62.3	−70.0 ± 10
MoO_3	419.59	−1.27	−5.33	−0.67	412.32	−78.3	−79.3	−82.8 ± 5
WO_3	473.98	−1.01	−5.38	−0.67	458.48	−78.5	−79.6	−70.0 ± 7
Ti_2O_4	719.98	+7.49	−8.67	−2.16	716.64	−255.9	−257.7	−265.6 ± 11[i] −262.2 ± 11[i]
Zr_2O_4	790.69	+7.44	−7.65	−5.02	785.46	−261.7	−263.5	
Hf_2O_4	799.33	+4.15	−7.54	−16.58	779.36	−248.0	−249.9	
Cr_2O_6	772.96	+1.28	−13.66	−1.34	759.24	−216.4	−218.8	
Mo_2O_6	951.42	−0.04	−12.38	−1.34	937.66	−269.6	−271.8	−280.8 ± 13[i]
W_2O_6	1076.66	−0.82	−12.12	−1.34	1045.50	−285.5	−287.8	−278.2 ± 10

[a] ΔE_{Val}(DK) from Table 1 for M = Ti and Cr, and $\Delta E_{Val,corr}$(PP) for M = Zr, Hf, Mo, and W from Table 1. [b] Calculated from the CCSD(T)-DK/awCVTZ-DK energy differences with and without correlating the metal $(n-1)s^2(n-1)p^6$ (n = 3 for Ti and Cr, n = 4 for Zr and Mo, n = 5 for W) and oxygen $1s^2$ electrons. For M = W, the metal $4f^{14}$ electrons were also correlated. For M = Hf, calculated from the CCSD(T)/awCVTZ-PP energy differences with and without correlating the metal $5s^25p^6$ and oxygen $1s^2$ electrons. [c] BP86/aVDZ-PP. [d] Experimental atomic spin−orbit corrections from ref 58 (−0.22, −0.64, −2.06, and −7.84 kcal/mol for O, Ti, Zr, and Hf, and 0 kcal/mol for Cr, Mo, and W). [e] $\Sigma D_{0,0K} = \Delta E_{Val} + \Delta E_{CV} + \Delta E_{ZPE} + \Delta E_{SO}$. For M = W, it was corrected by the energy difference between the $^7S_3$ and $^5D_0$ states (8.44 kcal/mol). [f] Equation 10: $\Delta H_{f,\ 0K}[(MO_m)_n] = n\Delta H_{f,0K}(M) + m{*}n\Delta H_{f,0K}(O) - \Sigma D_{0,0K}[(MO_m)_n]$. $\Delta H_{f,0K}$ is 58.98 ± 0.02 kcal/mol for O, 112.4 ± 0.7 kcal/mol for Ti, 143.9 ± 2.0 kcal/mol for Zr, 147.7 ± 1.5 kcal/mol for Hf, 94.5 ± 1.0 kcal/mol for Cr, 157.1 ± 0.9 kcal/mol for Mo, and 203.1 ± 1.5 kcal/mol for W. [g] $\Delta H_{f,298K}[(MO_m)_n] = \Delta H_{f,0K}[(MO_m)_n] + \Delta H_{0K\rightarrow298K}[(MO_m)_n] - n\Delta H_{0K\rightarrow298K}(Ti) - n{*}m\Delta H_{0K\rightarrow298K}(O)$. $\Delta H_{0K\rightarrow298K}$ is 1.04 kcal/mol for O, 1.15 kcal/mol for Ti, 1.31 kcal/mol for Zr, 1.40 kcal/mol for Hf, 0.97 kcal/mol for Cr, 1.10 kcal/mol for Mo, and 1.19 kcal/mol for W. The enthalpy change from 0 to 298 K for the cluster is calculated at the BP86/aVDZ-PP level. [h] Reference 59a. [i] Derived values based on refs 61−63. See text.

few kcal/mol in the calculated TAEs. It is clear that experimental measurements of highly accurate energetics for transition metal compounds, especially of heats of formation of atoms and molecules are needed to provide accurate benchmarks of the computational approaches.

Table 3 gives the additional energy terms needed to calculate the TAEs and the corresponding heats of formation. The core−valence corrections to the TAEs calculated at the CCSD(T)-DK/awCVTZ-DK level are to increase the TAEs for Cr_2O_6 by ∼1.3 kcal/mol, for TiO_2 and ZrO_2 by ∼2.9 kcal/mol, and for Ti_2O_4 and Zr_2O_4 by ∼7.5 kcal/mol. In contrast, they decrease the TAEs for CrO_3, MoO_3, WO_3, and W_2O_6 by 0.6−1.3 kcal/mol. For Mo_2O_6, the core−valence correction is negligibly small. The core−valence corrections to the TAEs calculated at the CCSD(T)/awCVTZ-PP level given in the Supporting Information are larger than those calculated at the CCSD(T)-DK/awCVTZ-DK level by ∼0.4 kcal/mol for TiO_2 and W_2O_6, by ∼2 kcal/mol for MoO_3 and Ti_2O_4, ∼4 kcal/mol for CrO_3 and Mo_2O_6, and ∼8 kcal/mol for Cr_2O_6. For ZrO_2 and Zr_2O_4, they are smaller by ∼0.6 and 0.2 kcal/mol, respectively. For WO_3, they are essentially the same. As might be expected, the core−valence corrections to the TAEs are better calculated at the CCSD(T)-DK level especially for M = Cr and Mo.

Our recent studies on the $(TiO_2)_n$ (n = 1−4) clusters[17d] revealed a strong basis set dependence of their TAEs calculated at the CCSD(T) level. As shown in Tables 1 and 2, for the monomers the basis set extrapolation effects at the CCSD(T) level from aVDZ-PP to CBS are ∼19 kcal/mol for TiO_2, 24−25 kcal/mol for ZrO_2 and HfO_2, ∼28 kcal/mol for CrO_3, and 38−40 kcal/mol for MoO_3 and WO_3. Those from aVTZ-PP to CBS are still substantial, 8−9 kcal/mol for TiO_2, ZrO_2, and HfO_2, ∼11 kcal/mol for CrO_3, and 13−14 kcal/mol for MoO_3 and WO_3. The variation in the basis set extrapolation effects from aVTZ-PP to CBS is considerably smaller than that from aVDZ-PP to CBS. For the dimers, the basis set extrapolation effects from aVTZ-PP to CBS are nearly twice as large as those for the monomers. Similar conclusions are reached for the basis set extrapolation effects calculated at the CCSD(T)-DK level with the DK basis sets for M = Ti and Cr (Table 1). Thus, to calculate the TAEs directly at the CCSD(T) level, one needs to use very large basis sets to extrapolate to the CBS limit. This is currently only possible for relatively small systems. To obtain "chemical accuracy" for the calculated heats of formation from the TAEs for these clusters at the CCSD(T) level, the valence electronic energies need to be calculated at the CCSD(T)/CBS level with the RECP basis sets and for some systems at the CCSD(T)-DK/CBS level, and the core−valence corrections need to be evaluated at the CCSD(T)-DK/awCVTZ-DK level. For larger clusters, this becomes computationally unattainable. We have recently developed an efficient approach[17d] to calculate the heats of formation for large clusters using the clustering energies, which will be further discussed below.

Heats of Formation of Monomers and Dimers. Table 3 also presents the calculated TAEs at 0 K at the CCSD(T)-DK level or at CCSD(T) level with pseudopotential corrections and the derived heats of formation at 0 and 298 K and compares them to available experimental heats of formation at 298 K. The TAEs and heats of formation calculated at the CCSD(T) level without the pseudopotential correction are included as Supporting Information. There is a lack of accurate experimental heats of formation for transition metal compounds. As accurate experimental values are crucial for our benchmark study, we have analyzed heats of formation data not available in the JANAF tables and the CODATA recommended key values.[59] For TiO_2, high temperature mass spectroscopic measurement by Balducci et al.[61] yielded a value of 301.1 ± 3 kcal/mol for the TAE. Using the CODATA recommended heats of formation for Ti and O,[59b] we derived a value of −71.4 ± 3 kcal/mol for the heat of formation at 298 K for TiO_2, compared to the adopted value of −73.0 ± 3 kcal/mol in the JANAF tables.[59a] For Ti_2O_4, Balducci et al.[62] determined the dimerization energy of TiO_2 at 0 K as -118.8 ± 10 kcal/mol, which yields the heat of formation at 298 K for the dimer as -265.6 ± 11 kcal/mol using the JANAF value for the heat of formation for TiO_2 and -262.2 ± 11 kcal/mol using our derived value for the heat of formation for TiO_2. For Mo_2O_6 and Mo_3O_9, Burns et al.[63] determined the dimerization and trimerization energies of MoO_3 at 1600 K to be -110.2 ± 8 and -222.8 ± 13 kcal/mol, respectively, from which we derived the heats of formation at 298 K for the dimer and trimer of -280.8 ± 13 and -481.5 ± 19 kcal/mol, respectively, by correcting the reaction enthalpies from 1600 to 298 K with the appropriate corrections obtained at the BP86/aVDZ-PP level and using the heat of formation for the monomer from the JANAF tables. We note that the adopted JANAF value for the heat of formation for MoO_3 was derived from the above work of Burns et al.[63] In addition, Norman and Staley[64] determined the dimerization and trimerization energies of MoO_3 and WO_3. However, as noted in the JANAF tables, the absolute pressures reported by Norman and Staley appear to be inconsistent with the JANAF functions, and thus we did not use their experimental data. For $(WO_3)_n$ ($n = 1-4$), we used the adopted experimental heats of formation from the JANAF tables.

As shown in Table 3, for the monomers, the heats of formation calculated at 298 K calculated are less negative than the experimental values by ~1.0 kcal/mol for ZrO_2, by ~3.5 kcal/mol for TiO_2, which falls slightly outside the error limit of our derived experimental value, by ~3.5 kcal/mol for MoO_3, and by ~7.7 kcal/mol for CrO_3. For WO_3, the calculated value is ~9.6 kcal/mol more negative than the experimental one. The calculated values are all essentially within the experimental error limits except for WO_3. Compared to the heats of formation calculated at the CCSD(T)-DK level or at the CCSD(T) level with the pseudopotential corrections, those calculated at the CCSD(T) level without the pseudopotential corrections (Supporting Information) differ more from the experimental values for ZrO_2 and MoO_3, and less for CrO_3. For TiO_2 and WO_3, they are of similar quality. For the dimers, the experimental heats of formation are available only for M = Ti, Mo, W, and the CCSD(T)-DK or corrected CCSD(T) values lie within the experimental error bars for all three clusters. The calculated values for Ti_2O_4 and Mo_2O_6 are less negative and that for W_2O_6 is more negative than the experimental values, as expected on the basis of the monomers. For Mo_2O_6 and W_2O_6, the corrected CCSD(T) values are in better agreement with the experimental values than the uncorrected CCSD(T) results.

Normalized Clustering Energies. Due to the strong basis set dependence of the TAEs and thus the heats of formation derived from the TAEs at the CCSD(T) level for these oxide clusters, it is desirable to find an approach to substantially reduce the basis set dependence in the calculated TAEs or heats of formation for the larger clusters. In our recent work on the titanium oxide clusters,[17d] we showed that an improved way to calculate the heats of formation for the larger clusters is to use the normalized clustering energies (NCEs), as the NCEs are much less basis set dependent than the TAEs. An additional advantage of this approach is the possibility of calculating the NCEs at reasonable accuracy with other more computationally efficient theoretical methods, for example with DFT. This approach resembles of isodesmic approach widely employed in computational organic and main group thermochemistry.[27]

Similar to the calculations for the TAEs, the NCEs for the dimers, trimers, and tetramers were calculated as sums of the different energy components: the valence electronic energy contribution with the scalar relativistic and pseudopotential corrections (Tables 4−6), the core−valence correction (Table 7), and the ZPE correction (Table 8). For the dimers, the valence electronic energy was evaluated at the CCSD(T)/CBS or CCSD(T)-DK/CBS level, whereas for the trimers and tetramers, it was evaluated up to the CCSD(T)/aVTZ-PP or CCSD(T)-DK/aVTZ-DK level.

For the dimers, the calculated pseudopotential corrections to the NCEs from eq 3 are small, 0.2−0.4 kcal/mol for Ti_2O_4 and Cr_2O_6. The valence electronic energy contributions calculated at the CCSD(T)-DK/CBS level with the DK basis sets, and those calculated at the CCSD(T)/CBS level with RECP basis sets and corrected with the pseudopotential errors are also in agreement within 0.1 kcal/mol. The pseudopotential corrections for the dimers of Zr_2O_4, Hf_2O_4, Mo_2O_6, and W_2O_6 are all small, less than 0.4 kcal/mol.

For the trimers and tetramers, the estimated pseudopotential corrections are also small, less than 0.5 kcal/mol. The scalar relativistic corrections to the NCEs calculated as the MVD expectation values at the CISD/aVTZ-PP level are to decrease the NCEs by 0.1−0.2 kcal/mol for M = Zr and Hf, and by 0.4−0.5 kcal/mol for M = Ti. Those calculated at the HF/aVTZ-PP level are less negative by ~0.1 kcal/mol for M = Zr and Hf, and ~0.2 kcal/mol for M = Ti. Compared to those for the dimers, the scalar relativistic corrections to the NCEs for the trimers and tetramers are only slightly more negative by up to 0.2 kcal/mol for M = Ti, Zr, and Hf. Compared to the valence electronic energy contributions calculated at the CCSD(T)-DK/aVTZ-DK level, those calculated at the CCSD(T)/aVTZ-PP level are essentially the same for Zr_3O_6, and they are slightly smaller by 0.3−0.4 kcal/mol for Ti_3O_6 and Ti_4O_8, and slightly larger by ~0.3 kcal/mol for Zr_4O_8. For Hf_3O_6 and Hf_4O_8, the NCEs were calculated only at the CCSD(T) level with the RECP basis sets. For the trimers and tetramers for M = Cr, Mo, and W, the scalar relativistic corrections were only calculated at the

TABLE 4: Valence Electronic Energy Contributions to the Normalized Clustering Energies at 0 K in kcal/mol for the Ground States of $(TiO_2)_2$ and $(CrO_3)_2$ Calculated at the CCSD(T) Level with the Pseudopotential Corrections and at the CCSD(T)-DK Level[a]

	molecule			
	Ti_2O_4		Cr_2O_6	
	PP	DK	PP	DK
$\Delta E_{\mathrm{n=D}}$[b]	60.69	60.45	45.64	46.89
$\Delta E_{\mathrm{n=T}}$[c]	60.85	60.79	46.75	46.70
$\Delta E_{\mathrm{n=Q}}$[c]	60.96	60.87	46.69	46.65
ΔE_{CBS}[d]	61.03	60.91	46.61	46.61
ΔE_{SR}[c,e]	−0.31		−0.43	
ΔE_{Val}[f]	60.72	60.91	46.18	46.61
$\Delta E_{\mathrm{awCVTZ}}$[c,g]	60.56	60.52	46.49	46.45
$\Delta E_{\mathrm{PP,corr}}$[h]	+0.27		+0.39	
$\Delta E_{\mathrm{Val,corr}}$[i]	60.99		46.57	
$\Delta\Delta E_{\mathrm{Val}}$[j]	+0.08		−0.04	

[a] Each term was calculated from eq 5. [b] Geometries from CCSD(T)/aVDZ-PP. [c] Geometries from CCSD(T)/aVTZ-PP. [d] Extrapolated CCSD(T) or CCSD(T)-DK energies with n = D, T, and Q using eq 1. [e] MVD expectation values of the CISD/aVTZ-PP wave function. [f] $\Delta E_{\mathrm{Val}}(\mathrm{PP}) = \Delta E_{\mathrm{CBS}}(\mathrm{PP}) + \Delta E_{\mathrm{SR}}$, and $\Delta E_{\mathrm{Val}}(\mathrm{DK}) = \Delta E_{\mathrm{CBS}}(\mathrm{DK})$. [g] Valence electronic energies calculated at the CCSD(T)/awCVTZ-PP and CCSD(T)-DK/awCVTZ-DK levels. [h] Equation 3: $\Delta E_{\mathrm{PP,corr}} = \Delta E_{\mathrm{awCVTZ\text{-}DK}} - (\Delta E_{\mathrm{awCVTZ\text{-}PP}} + \Delta E_{\mathrm{SR}})$. [i] Equation 4: $\Delta E_{\mathrm{Val,corr}}(\mathrm{PP}) = \Delta E_{\mathrm{Val}}(\mathrm{PP}) + \Delta E_{\mathrm{PP,corr}} = \Delta E_{\mathrm{CBS}}(\mathrm{PP}) + \Delta E_{\mathrm{awCVTZ\text{-}DK}} - \Delta E_{\mathrm{awCVTZ\text{-}PP}}$. [j] $\Delta\Delta E_{\mathrm{Val}} = \Delta E_{\mathrm{Val,corr}}(\mathrm{PP}) - \Delta E_{\mathrm{Val}}(\mathrm{DK})$.

TABLE 5: Valence Electronic Energy Contributions to the Normalized Clustering Energies at 0 K in kcal/mol for the Ground States of $(MO_2)_2$ and $(M'O_3)_2$ (M = Zr, Hf; M′ = Mo, W) Calculated at the CCSD(T) Level with the Pseudopotential Corrections[a]

molecule	$\Delta E_{n=D}$[b]	$\Delta E_{n=T}$[c]	$\Delta E_{n=Q}$[c]	ΔE_{CBS}[d]	ΔE_{SR}[c,e]	ΔE_{Val}[f]	$\Delta E_{awCVTZ\text{-}PP}$[c,g]	$\Delta E_{awCVTZ\text{-}DK}$[c,h]	$\Delta E_{PP,corr}$[i]	$\Delta E_{Val,corr}$[j]
Zr_2O_4	64.70	64.10	64.19	64.28	−0.12	64.16	63.64	63.65	+0.13	64.29
Hf_2O_4	75.03	74.72	74.85	74.95	−0.11	74.84	75.54	75.09	−0.34	74.50
Mo_2O_6	55.36	56.13	56.12	56.08	−0.15	55.93	55.74	55.78	+0.19	56.12
W_2O_6	63.34	64.32	64.40	64.43	−0.15	64.28	63.91	63.84	+0.08	64.36

[a] Each term was calculated from eq 4. [b] Geometries from CCSD(T)/aVDZ-PP. [c] Geometries from CCSD(T)/aVTZ-PP. [d] Extrapolated CCSD(T) energies with n = D, T, and Q using eq 1. [e] MVD Expectation values of the CISD/aVTZ-PP wave function. [f] $\Delta E_{Val}(PP) = \Delta E_{CBS}(PP) + \Delta E_{SR}$. [g] Valence electronic energies calculated at the CCSD(T)/awCVTZ-PP level. For M = Hf, the metal $5s^25p^6$ and oxygen $1s^2$ electrons were also correlated. [h] Valence electronic energies at the CCSD(T)-DK/awCVTZ-DK level. For M = Hf, the metal $5s^25p^64f^{14}$ and oxygen $1s^2$ electrons were also correlated. [i] $\Delta E_{PP,corr} = \Delta E_{awCVTZ\text{-}DK} - [\Delta E_{awCVTZ\text{-}PP} + \Delta E_{SR}]$. [j] $\Delta E_{Val,corr}(PP) = \Delta E_{Val}(PP) + \Delta E_{PP,corr} = \Delta E_{CBS}(PP) + \Delta E_{awCVTZ\text{-}DK} - \Delta E_{awCVTZ\text{-}PP}$.

TABLE 6: Valence Electronic Energy Contributions to the Normalized Clustering Energies at 0 K in kcal/mol for the Ground States of $(MO_2)_n$ and $(M'O_3)_n$ (M = Ti, Zr, Hf; M′ = Cr, Mo, W; *n* = 3, 4) Calculated at the CCSD(T) and CCSD(T)-DK Levels[a]

molecule	basis	$\Delta E_{n=D}$[b]	$\Delta E_{n=T}$[b]	ΔE_{SR}[b,c]	$\Delta E_{SR,HF}$[b,d]	ΔE_{Val}[e]	$\Delta E_{PP,corr}$[f]
Ti_3O_6	PP	82.85	82.95	−0.42	−0.24	82.53	+0.33
	DK	82.82	82.86			82.86	
Zr_3O_6	PP	88.16	87.47	−0.17	−0.09	87.30	+0.02
	DK		87.32			87.32	
Hf_3O_6	PP	101.11	100.60	−0.14	−0.07	100.46	
Cr_3O_9	PP	54.94	56.44		−0.28	56.16	+0.22
	DK	57.06	56.38			56.38	
Mo_3O_9	PP	68.18	69.78		−0.10	69.68	+0.01
	DK		69.69			69.69	
W_3O_9	PP	80.18	81.97		−0.10	81.87	−0.41
	DK		81.46			81.46	
Ti_4O_8	PP	95.29	95.57	−0.53	−0.32	95.04	+0.43
	DK	95.30	95.47			95.47	
Zr_4O_8	PP	105.26	104.50	−0.21	−0.11	104.29	−0.26
	DK		104.03			104.03	
Hf_4O_8	PP	120.63	120.04	−0.18	−0.09	119.86	
Cr_4O_{12}	PP	57.51	59.21		−0.30	58.91	+0.23
	DK	59.74	59.14			59.14	
Mo_4O_{12}	PP	71.02	72.99		−0.11	72.88	−0.01
	DK		72.87			72.87	
W_4O_{12}	PP	83.60	85.97			85.97	

[a] Each term was calculated from eq 4. [b] Geometries from B3LYP/aVDZ-PP. [c] MVD Expectation values of the CISD/aVTZ-PP wave function. [d] MVD Expectation values of the HF/aVTZ-PP wave function. [e] $\Delta E_{Val}(PP) = \Delta E_{n=T}(PP) + \Delta E_{SR}$ and $\Delta E_{Val}(DK) = \Delta E_{n=T}(DK)$. For $(M'O_3)_n$, $\Delta E_{SR,HF}$ was used. [f] $\Delta E_{PP,corr} = \Delta E_{aVTZ\text{-}DK} - [\Delta E_{aVTZ\text{-}PP} + \Delta E_{SR}]$. For $(M'O_3)_n$, $\Delta E_{SR,HF}$ was used.

HF/aVTZ-PP level due to limitations of the MOLPRO program. Compared to the valence electronic energy contributions calculated at the CCSD(T)-DK/aVTZ-DK level, those calculated at the CCSD(T)/aVTZ-PP level are essentially the same for Mo_3O_9 and Mo_4O_{12}, slightly smaller by ∼0.2 kcal/mol for Cr_3O_9 and Cr_4O_{12}, and slightly larger by ∼0.4 kcal/mol for W_3O_9. For W_4O_{12}, the NCE were calculated only at the CCSD(T) level with the RECP basis sets.

For the dimers, trimers, and tetramers, the valence electronic energy contributions to the NCEs calculated at the CCSD(T)/CBS level for the dimers and at the CCSD(T)/aVTZ-PP level for the trimers and tetramers without the scalar relativistic corrections agree with those calculated at the CCSD(T)-DK level within 0.1 kcal/mol except for W_2O_6, Zr_3O_6, W_3O_9, and Zr_4O_8, where the differences range from 0.2 to 0.5 kcal/mol, and for Hf_2O_6, Hf_3O_6, Hf_4O_8, and W_4O_{12}, where the CCSD(T)-DK values are not available.

For the dimers, the basis set extrapolation effects for the NCEs from aVDZ-PP to CBS are calculated to increase them by ∼0.3 kcal/mol for Ti_2O_4, ∼0.7 kcal/mol for Mo_2O_6, and ∼1 kcal/mol for Cr_2O_6 and W_2O_6. For Zr_2O_4, the extrapolation decreases the NCE by ∼0.4 kcal/mol, and for Hf_2O_4, the extrapolation effect is negligibly small. Compared to the basis set extrapolation effects for the TAEs, those for the NCEs are smaller by 2−3 orders of magnitude. Furthermore, the basis set extrapolation effects from aVTZ-PP to CBS for these NCEs are less than 0.2 kcal/mol. Thus, the valence electronic energy contributions to the NCEs calculated with the aVTZ-PP basis sets for the dimers are reasonably well converged with respect to the CBS limit. Similar conclusions were reached for the basis set extrapolation effects to the NCEs calculated at the CCSD(T)-DK level for Ti_2O_4 and Cr_2O_6, except that for Cr_2O_6, the NCE calculated at the CCSD(T)-DK/aVDZ-DK level are ∼0.3 kcal/mol larger than that at the CCSD(T)-DK/CBS level. Our results show that basis set superposition errors (BSSE) are small for the NCEs of the dimer, and the NCEs calculated at the CCSD(T) or CCSD(T)-DK level with the aVDZ-PP or aVDZ-DK basis sets are accurate to ∼1 kcal/mol and those calculated with the aVTZ-PP or aVTZ-DK basis sets are accurate to ∼0.2 kcal/mol with respect to the CBS limit.

For the trimers and tetramers, the NCEs calculated at the CCSD(T)/aVDZ-PP level are smaller than those calculated at the CCSD(T)/aVTZ-PP level by 0.1−0.3 kcal/mol for Ti_3O_6 and Ti_4O_8, and by 1.5−2.5 kcal/mol for M = Cr, Mo, and W. For M = Zr and Hf, the NCEs calculated at the CCSD(T)/aVDZ-PP level are larger than those calculated at the CCSD(T)/

TABLE 7: Core−Valence Corrections to the Normalized Clustering Energies at 0 K in kcal/mol for the Ground States of $(MO_2)_n$ and $(M'O_3)_n$ (M = Ti, Zr, Hf; M′ = Cr, Mo, W; $n = 2-4$) Calculated at the CCSD(T) and CCSD(T)-DK Levels[a]

molecule	basis	wCVDZ	awCVDZ	wCVTZ	awCVTZ
Ti_2O_4	PP	+2.07	+2.54	+1.38	+1.60
	DK			+0.61	+0.82
Zr_2O_4	PP	+1.91	+2.78	+1.05	+1.37
	DK			+0.57	+0.83
Hf_2O_4	PP	+1.08	+1.72	+0.92	+1.27
Cr_2O_6	PP	+1.93	+2.54	+1.57	+1.82
	DK			+1.06	+1.28
Mo_2O_6	PP	+1.82	+2.59	+1.41	+1.74
	DK			+1.01	+1.25
W_2O_6	PP	+0.78	+1.52	+0.38	+0.72
	DK			+0.25	+0.60
Ti_3O_6	PP	+3.07	+3.84	+2.29	
	DK			+1.25	
Zr_3O_6	PP	+2.86	+4.34	+1.84	
	DK			+1.17	
Hf_3O_6	PP	+1.71	+2.67	+1.54	
Cr_3O_9	PP	+2.11	+2.74	+1.81	
	DK			+1.20	
Mo_3O_9	PP	+1.94	+2.93	+1.52	
	DK			+1.07	
W_3O_9	PP	+0.90	+1.82	+0.61	
	DK			+0.56	
Ti_4O_8	PP	+3.80	+4.79	+2.62	
	DK			+1.27	
Zr_4O_8	PP	+3.31	+5.22	+1.86	
	DK			+1.01	
Hf_4O_8	PP	+1.88	+3.06	+1.42	
Cr_4O_{12}	PP	+2.08	+2.81		
Mo_4O_{12}	PP	+1.95	+3.06		
W_4O_{12}	PP	+0.87	+1.84	+0.61	

[a] Each term was calculated from eq 4 using the CCSD(T) or CCSD(T)-DK energy differences with and without correlating the metal $(n-1)s^2(n-1)p^6$ ($n = 3$ for Ti and Cr, $n = 4$ for Zr and Mo, $n = 5$ for Hf and W) and oxygen $1s^2$ electrons. For the CCSD(T)-DK calculations for M = W, the metal $4f^{14}$ electrons were also correlated.

aVTZ-PP level by 0.5−0.8 kcal/mol. The NCEs calculated at the CCSD(T)-DK/aVDZ-DK level are up to 0.3 kcal/mol smaller than those calculated at the CCSD(T)-DK/aVTZ-DK level for M = Ti, but the former are 0.6−0.7 kcal/mol larger than the latter for M = Cr. Thus, for the trimers and tetramers for M = Cr, Mo, and W, errors on the order of 2 kcal/mol in the NCEs arise when calculated at the CCSD(T)/aVDZ-PP level as compared to either the CCSD(T)/aVTZ-PP or CCSD(T)-DK/aVTZ-DK levels.

Table 7 compares the core−valence corrections to the NCEs calculated at the various level of theory. For the dimers, the core−valence correction was calculated at the CCSD(T) level with the awCVnZ-PP and wCVnZ-PP (n = D, T) basis sets, and at the CCSD(T)-DK level with the awCVTZ-DK and wCVTZ-DK basis sets. The core−valence corrections to the NCEs calculated at the CCSD(T)-DK/awCVTZ-DK level are to increase them by ~0.6 kcal/mol for W_2O_6, ~0.8 kcal/mol for Ti_2O_4 and Zr_2O_4, and ~1.3 kcal/mol for Cr_2O_6 and Mo_2O_6. For Hf_2O_4, the core−valence correction was not calculated separately at the CCSD(T)-DK level due to the problem with Hf mentioned above. The core−valence corrections to the NCEs calculated at the CCSD(T)-DK/wCVTZ-DK level are smaller than those calculated at the CCSD(T)-DK/awCVTZ-DK level by 0.2−0.3 kcal/mol. On the other hand, the core−valence corrections calculated at the CCSD(T)/awCVTZ-PP level are larger than those calculated at the CCSD(T)-DK/awCVTZ-DK level by ~0.1 kcal/mol for W_2O_6, ~0.5 kcal/mol for Zr_2O_4, Cr_2O_6, and Mo_2O_6, and ~0.8 kcal/mol for Ti_2O_4. The reason that the core−valence corrections calculated at the CCSD(T)/awCVTZ-PP and CCSD(T)-DK/awCVTZ-DK level for W_2O_6 are closer to each other than those for M = Ti, Cr, Zr, and Hf might be partially due to the additional correlation effect of the W 4f electrons at the CCSD(T)-DK level, whereas it was not explicitly included at the CCSD(T)/awCVTZ-PP level. In addition, the core−valence corrections to the NCEs calculated at the CCSD(T) or CCSD(T)-DK level with the different basis sets follow the order of awCVDZ-PP > wCVDZ-PP > awCVTZ-PP > wCVTZ-PP > awCVTZ-DK > wCVTZ-DK except for Hf_2O_4 where awCVTZ-PP > wCVDZ-PP and W_2O_6 where awCVTZ-DK > wCVTZ-PP. The core−valence corrections calculated at the CCSD(T)/wCVTZ-PP level are larger than those calculated at the CCSD(T)-DK/awCVTZ-DK level by 0.2−0.3 kcal/mol for M = Zr, Cr, and Mo, and by ~0.6 kcal/mol for M = Ti, but it is smaller by ~0.2 kcal/mol for M = W. The core−valence corrections calculated at the CCSD(T)/wCVDZ-PP level are larger than those calculated at the CCSD(T)-DK/awCVTZ-DK level by ~0.2 kcal/mol for M = W, 0.6−0.7 kcal/mol for M = Cr and Mo, and 1.1−1.3 kcal/mol for M = Ti and Zr.

For the trimers and tetramers, the core−valence corrections to the NCEs calculated at the CCSD(T)/wCVTZ-PP level are larger than those calculated at the CCSD(T)-DK/wCVTZ-DK level by 0.5−0.7 kcal/mol for Zr_3O_6, Cr_3O_9, and Mo_3O_9, 0.9−1.0 kcal/mol for Ti_3O_6 and Zr_4O_8, and ~1.4 kcal/mol for Ti_4O_8. For W_3O_9, the core−valence corrections to the NCEs calculated at the CCSD(T)/wCVTZ-PP and CCSD(T)-DK/wCVTZ-DK levels are essentially the same. The core−valence corrections to the NCEs calculated with the different basis sets follow an order similar to that for the dimers, awCVDZ-PP > wCVDZ-PP > wCVTZ-PP > wCVTZ-DK. Those calculated at the CCSD(T) /wCVDZ-PP level are overestimated by ~0.3 kcal/mol for W_3O_9, ~0.9 kcal/mol for Cr_3O_9 and Mo_3O_9, 1.7−1.8 kcal/mol for Ti_3O_6 and Zr_3O_6, and 2.3−2.5 kcal/mol for Ti_4O_8 and Zr_4O_8, with respect to the CCSD(T)-DK/wCVTZ-DK values.

On the basis of the above discussion, our best estimated core−valence corrections are in order of preference: awCVTZ-DK > wCVTZ-DK at the CCSD(T)-DK level, and wCVTZ-PP > awCVTZ-PP > wCVDZ-PP > awCVDZ-PP at the CCSD(T) level. The electronic energy contribution to the NCE can be calculated from the valence electronic energy contribution shown in Tables 4−6 and the best estimated core−valence correction in Table 7. The NCEs calculated at the CCSD(T)-DK level or at the CCSD(T) level with the pseudopotential corrections are given in Table 8, and those calculated without the pseudopotential corrections are given as Supporting Information. The effect of the pseudopotential corrections is small, <1.2 kcal/mol in the worst case.

Comparing to the calculations of the TAEs of these TMO clusters at the CCSD(T) level, the calculations of their NCEs are much easier due to the significantly reduced basis set effects for the valence electronic energies, as well as the smaller core−valence corrections. While the TAEs have to be calculated at the CCSD(T)-DK/CBS level and sometimes at the CCSD(T)/CBS level with the RECP basis sets, the NCEs can be evaluated at the CCSD(T)-DK/aVTZ-DK or CCSD(T)/aVTZ-PP level and those calculated at the CCSD(T)-DK/aVDZ-DK or CCSD(T)/aVDZ-PP level are reasonably accurate within 1 kcal/mol for the dimers and 2 kcal/mol for the trimers and tetramers. For

TABLE 8: Normalized Clustering Energies at 0 K (ΔE_{0K}, kcal/mol) for the Ground States of $(MO_2)_n$ and $(M'O_3)_n$ (M = Ti, Zr, Hf; M′ = Cr, Mo, W; $n = 2-4$) Calculated at the CCSD(T)-DK Level or at the CCSD(T) Level with the Pseudopotential Corrections[a] and Compared with Available Experimental Data

molecule	ΔE_{Val}[b]	ΔE_{CV}[c]	ΔE_{ZPE}[d]	ΔE_{0K}[e]	expt[f]		ΔE_{Val}[b]	ΔE_{CV}[c]	ΔE_{ZPE}[d]	ΔE_{0K}[e]	expt[f]
Ti_2O_4	60.91	+0.82	−1.08	60.7	59.4 ± 5[g]	Cr_2O_6	46.61	+1.28	−1.05	46.8	
Zr_2O_4	64.29	+0.83	−0.92	64.2		Mo_2O_6	56.12	+1.25	−0.85	56.5	57.5 ± 4[h]
Hf_2O_4	74.50	+1.27	−0.94	74.8		W_2O_6	64.36	+0.60	−0.68	64.3	69.4 ± 9
Ti_3O_6	82.86	+1.25	−1.34	82.8		Cr_3O_9	56.38	+1.20	−1.18	56.4	
Zr_3O_6	87.32	+1.17	−1.12	87.4		Mo_3O_9	69.69	+1.07	−0.98	69.8	77.7 ± 4[h]
Hf_3O_6	100.46	+1.54	−1.11	100.9		W_3O_9	81.46	+0.56	−0.88	81.1	91.3 ± 23
Ti_4O_8	95.47	+1.27	−1.48	95.3		Cr_4O_{12}	59.14	+2.08	−1.22	60.0	
Zr_4O_8	104.03	+1.01	−1.31	103.7		Mo_4O_{12}	72.87	+1.95	−0.92	73.9	
Hf_4O_8	119.86	+1.42	−1.29	120.0		W_4O_{12}	85.97	+0.61	−0.82	85.8	97.7 ± 30

[a] Each term was calculated from eq 4. [b] ΔE_{Val}(DK) from Table 4 for Ti_2O_4 and Cr_2O_6; $\Delta E_{Val,corr}$(PP) from Table 5 for Zr_2O_4, Hf_2O_4, Mo_2O_6, and W_2O_6; ΔE_{Val}(DK) from Table 6 for Ti_3O_6, Zr_3O_6, Cr_3O_9, Mo_3O_9, W_3O_9, Ti_4O_8, Zr_4O_8, and Cr_4O_{12}, Mo_4O_{12}; and ΔE_{Val}(PP) from Table 6 for Hf_3O_6, Hf_4O_8, and W_4O_{12}. [c] Calculated at the CCSD(T)-DK/awCVTZ-DK level for $n = 2$ and CCSD(T)-DK/wCVTZ-DK level for $n = 3$ and 4 (for Hf_2O_4, at the CCSD(T)/awCVTZ-PP level; for Hf_3O_6 and Hf_4O_8, at the CCSD(T)/wCVTZ-PP level; for Cr_4O_{12} and Mo_4O_{12}, at the CCSD(T)/wCVDZ-PP level). See Table 7. [d] BP86/aVDZ-PP. [e] $\Delta E_{0K} = \Delta E_{Val} + \Delta E_{CV} + \Delta E_{ZPE}$. [f] Reference 59a. [g] Reference 62. [h] Reference 63.

the TAEs, the core−valence corrections are best estimated at the CCSD(T)-DK/awCVTZ-DK level, especially for M = Cr and Mo (Table 3 and Supporting Information), whereas for the NCEs, they can be calculated at the CCSD(T)-DK/wCVTZ-DK or CCSD(T)/wCVTZ-PP level and those calculated at the CCSD(T)/wCVDZ-PP level are often reasonably accurate (Table 7). In addition, error cancellation may help improve the accuracy of the calculated NCE if the valence electronic energy is calculated at the CCSD(T)/aVDZ-PP level and the core−valence correction is calculated at the CCSD(T)/wCVDZ-PP level for M = Cr, Mo, and W. As shown in Table 6, for Cr_3O_9, Mo_3O_9, W_3O_9, Cr_4O_{12}, and Mo_4O_{12}, the valence electronic energy contributions to the NCEs calculated at the CCSD(T)/aVDZ-PP level are underestimated by 1.5−2.0 kcal/mol. The core−valence corrections to the NCEs (Table 7) calculated at the CCSD(T)/wCVDZ-PP level, on the other hand, are overestimated by 0.5−0.9 kcal/mol for Cr_3O_9 and Mo_3O_9, which partially compensates the underestimation of the valence electronic energy contributions. However, for M = Ti and especially for M = Zr, both valence electronic energy and core−valence correction tend to be overestimated at these lower levels of theory, which gives poorer results with this combination.

Although the NCEs of these clusters are much less basis set dependent than their TAEs, it is difficult to calculate them to within the "chemical accuracy" of 1 kcal/mol, especially for the large clusters. In addition, reaching the "chemical accuracy" of 1 kcal/mol for the NCEs for the large clusters is insufficient for achieving the same goal for their heats of formation, if one is to calculate the heats of formation based on eq 10, as there is a multiplicative factor. For the tetramer, an error in its NCE of 1 kcal/mol translates to 4 kcal/mol in its heat of formation calculated from eq 10, in addition to the error propagated from the heat of formation of the monomer. From Tables 4 and 5, the core−valence corrections to the NCEs are substantially larger than the basis set extrapolation effects from aVTZ-DK or aVTZ-PP to CBS, and they are larger or comparable to the basis set extrapolation effects from aVDZ-DK or aVDZ-PP to CBS. Thus, proper estimations of both the valence electronic energy contributions and the core−valence corrections are important in obtaining accurate NCEs.

Table 8 also compares the calculated NCEs at 0 K at the CCSD(T)-DK level or at the CCSD(T) level with the pseudopotential corrections to available experimental data. The NCEs at 0 K calculated at the CCSD(T) level without the pseudopotential corrections are included as Supporting Information. For the dimers, our calculated values at the CCSD(T)-DK or CCSD(T) level with all the corrections are within 1 kcal/mol from the experimental values for Ti_2O_4[62] and for Mo_2O_6.[63] For W_2O_6, although our calculated value at the CCSD(T) level with the pseudopotential correction is ~5 kcal/mol lower than the experimental value derived from the heats of formation of the monomer and dimer from the JANAF tables,[59](a) it is still well within the experimental error bar of 9 kcal/mol. For Mo_2O_6 and W_2O_6, our calculated NCEs at the CCSD(T) level with the pseudopotential corrections are only ~2 kcal/mol lower than the Norman and Staley values[64] of 58.8 and 66.5 kcal/mol respectively. For the trimers, our calculated NCEs at the CCSD(T)-DK/aVTZ-DK or CCSD(T)/aVTZ-PP level with all the corrections are lower than the experimental values by ~8 kcal/mol for Mo_3O_9[63] and ~10 kcal/mol for W_3O_9 derived from the heats of formation of the monomer and trimer from the JANAF tables.[59a] However, for both clusters, our calculated values are only ~4 kcal/mol lower than the Norman and Staley values[64] of 73.6 and 84.0 kcal/mol, respectively. For W_4O_{12}, although our calculated value at the CCSD(T)/aVDZ-PP level with all the corrections are lower than the experimental value derived from the JANAF tables[59a] by ~12 kcal/mol, it is still well within its large error of 30 kcal/mol. The above comparison may indicate that the dimerization and trimerization energies measured by Norman and Staley[64] for MoO_3 and WO_3 are reasonably accurate, contrary to the conclusions drawn in the JANAF tables.

Heats of Formation of Trimers and Tetramers. Table 9 presents the calculated heats of formation of the trimers and tetramers at 0 and 298 K at the CCSD(T)-DK or CCSD(T) level with the pseudopotential corrections from eq 10, and compares them with available experimental values at 298 K. The heats of formation calculated at the CCSD(T) level with the RECP basis sets are given as Supporting Information. For Mo_3O_9, our calculated heat of formation at 298 K at the CCSD(T) level of 447.3 kcal/mol are to be compared with the experimental values of 481.5 ± 19 kcal/mol derived from the trimerization energy of the monomer from Balducci et al.,[62] and 469.2 ± 15 kcal/mol derived from the trimerization energy from Norman and Staley,[64] in combination with the experimental heat of formation of the monomer from the JANAF tables.[59a] The error bar for the latter experimental value does not include the error associated with the trimerization energy from Norman and Staley,[64] which was not reported. Thus our calculated value is in fact

TABLE 9: Heats of Formation at 0 and 298 K ($\Delta H_{f,0K}$ and $\Delta H_{f,298K}$, kcal/mol) for the Ground States of $(MO_2)_n$ and $(M'O_3)_n$ (M = Ti, Zr, Hf; M′ = Cr, Mo, W; *n* = 3, 4) Calculated at the CCSD(T)-DK Level or at the CCSD(T) Level with the Pseudopotential Corrections from the Calculated Normalized Clustering Energies and Heats of Formation[a] and Compared with Available Experimental Data

	$\Delta H_{f,0K}$CCSD(T)[b]	$\Delta H_{f,298K}$CCSD(T)[c]		$\Delta H_{f,0K}$CCSD(T)[b]	$\Delta H_{f,298K}$CCSD(T)[c]	$\Delta H_{f,298K}$expt[d]
Ti_3O_6	−450.3	−453.1	Cr_3O_9	−353.4	−356.8	
Zr_3O_6	−462.3	−465.0	Mo_3O_9	−444.3	−447.3	−481.5 ± 19[e]
Hf_3O_6	−450.3	−453.2	W_3O_9	−478.8	−481.9	−483.6 ± 10
Ti_4O_8	−650.4	−654.5	Cr_4O_{12}	−485.6	−490.4	
Zr_4O_8	−681.6	−685.5	Mo_4O_{12}	−608.8	−612.8	
Hf_4O_8	−676.8	−680.8	W_4O_{12}	−657.2	−660.7	−670.2 ± 10

[a] Error bars due to errors in the experimental heats of formation of the atoms are ±0.7*n* for $(TiO_2)_n$, ±2.0*n* for $(ZrO_2)_n$, ±1.5*n* for $(HfO_2)_n$, ±1.0*n* for $(CrO_3)_n$, ±0.9*n* for $(MoO_3)_n$, and ±1.5*n* for $(WO_3)_n$ kcal/mol. [b] Equation 11: $\Delta H_{f,0K}[(MO_m)_n] = n\Delta H_{f,0K}(MO_m) - n\Delta E_{norm,n}[(MO_m)_n]$, using calculated heats of formation of the monomers from Table 3, and calculated normalized clustering energies from Table 8. [c] $\Delta H_{f,298K}[(MO_m)_n] = \Delta H_{f,0K}[(MO_m)_n] + \Delta H_{0K\rightarrow 298K}[(MO_m)_n] - n\Delta H_{0K\rightarrow 298K}(Ti) - nm\Delta H_{0K\rightarrow 298K}(O)$. $\Delta H_{0K\rightarrow 298K}$ is 1.04 kcal/mol for O, 1.15 kcal/mol for Ti, 1.31 kcal/mol for Zr, 1.40 kcal/mol for Hf, 0.97 kcal/mol for Cr, 1.10 kcal/mol for Mo, and 1.19 kcal/mol for W. The enthalpy change from 0 to 298 K for the cluster is calculated at the BP86/aVDZ-PP level. [d] Reference 59a. [e] Derived values based on ref 63. See text.

TABLE 10: Estimated M═O and M—O (M = Ti, Zr, Hf, Cr, Mo, W) Bond Energies at 0 K in kcal/mol from the Total Atomization Energies of the Monomers and Dimers Calculated at the CCSD(T)-DK or CCSD(T) Level[a]

	M = Ti	M = Zr	M = Hf	M = Cr	M = Mo	M =W
M═O[b]	148.8	164.3	157.4	110.9	137.4	152.8
M—O[c]	104.7	114.2	116.1	78.9	97.0	108.5

[a] From Table 3. [b] $^1/_2\Sigma D_{0,0K}(MO_2)$ for M = Ti, Zr, Hf and $^1/_3\Sigma D_{0,0K}(MO_3)$ for M = Cr, Mo, W. [c] $^1/_4[\Sigma D_{0,0K}(M_2O_4) - \Sigma D_{0,0K}(MO_2)]$ for M = Ti, Zr, Hf and $^1/_4[\Sigma D_{0,0K}(M_2O_6) - {}^4/_3\Sigma D_{0,0K}(MO_3)]$ for M = Cr, Mo, W.

TABLE 11: Differential Clustering Energies at 0 K (ΔE_{0K}, kcal/mol) for the Ground States of $(MO_2)_n$ and $(M'O_3)_n$ (M = Ti, Zr, Hf; M′ = Cr, Mo, W; *n* = 2−4) Calculated from the Heats of Formation at the CCSD(T)-DK or CCSD(T) Level[a]

	M = Ti	M = Zr	M = Hf	M′ = Cr	M′ = Mo	M′ = W
n = 2	121.3	128.3	149.6	93.6	113.0	128.5
n = 3	127.1	133.9	153.1	75.6	96.4	114.8
n = 4	132.8	152.6	177.3	70.8	86.2	99.9

[a] From Tables 3 and 9.

consistent with this latter experimental value. For W_3O_9, our CCSD(T) value of 481.9 kcal/mol is in excellent agreement with that adopted by the JANAF tables of 483.6 ± 10 kcal/mol. However, both values are much larger than the derived value of 461.8 kcal/mol from the heat of formation of the WO_3 in the JANAF tables and the trimerization energy reported by Norman and Staley.[64] For W_4O_{12}, our calculated value of 660.7 kcal/mol at 298 K is smaller by <10 kcal/mol than that adopted by the JANAF tables of 670.2 ± 10 kcal/mol, which is within the experimental error bar. The comparison between our calculated heats of formation and their experimental values for the limited set of data indicates that our approach can provide accurate heats of formation for the larger clusters, although more accurate experimental data are necessary for a better evaluation. In addition, the accuracy of the calculated NCE greatly affects the accuracy of the calculated heat of formation using eq 10 especially for large clusters.

Metal−Oxygen Bond Energies. Table 10 presents the estimated metal−oxygen bond energies at the CCSD(T)-DK level or at the CCSD(T) level with the pseudopotential corrections from the calculated TAEs of the monomers and dimers following our recent work.[17b,d] Those calculated at the CCSD(T) level without the pseudopotential corrections are included as Supporting Information. As the TAE of the monomer is the energy required to break the M═O bonds, the average M═O bond energy is half of the TAE for MO_2 (M = Ti, Zr, Hf), and one-third of that for MO_3 (M = Cr, Mo, W). By assuming the average M═O bond energy in the dimer is the same as that in the monomer, one can calculate the average M—O bridge bond energy as $^1/_4[\Sigma D_{0,0K}(M_2O_4) - \Sigma D_{0,0K}(MO_2)]$ for M = Ti, Zr, Hf, and $^1/_4[\Sigma D_{0,0K}(M_2O_6) - {}^4/_3\Sigma D_{0,0K}(MO_3)]$ for M = Cr, Mo, W. The estimated average M═O bond energy at the CCSD(T)-DK level or at CCSD(T) level with the pseudopotential corrections ranges from 110 to 165 kcal/mol and follows the order Cr < Mo < Ti < W < Hf < Zr. The larger M═O bond energy for the group IVB metal oxides than the group VIB metal oxides is likely due to increased ionic bonding character in the former, even though the latter have higher oxidation state. The bond energy increases with the atomic number for the group VIB metals. For the group IVB metals, the bond energy increases from Ti to Zr as expected but decreases from Zr to Hf. The estimated average M—O bond energy is less than that of M═O by ~30 kcal/mol for M = Cr and by 40−50 kcal/mol for the other metals and follows a similar order except for that between M = Zr and Hf. Both types of metal−oxygen bonds are very strong, consistent with the significant ionic nature of the bonding and the interaction between the filled O pπ orbitals and the empty M dπ orbitals.[65]

Differential Clustering Energies. Table 11 presents the differential clustering energies (DCEs) at 0 K calculated from the heats of formation at the CCSD(T)-DK or CCSD(T) level from Tables 3 and Tables 9. The DCE of $(MO_m)_n$, $\Delta E_{diff,n}$, is defined as[17a,d]

$$\Delta E_{diff,n} = E[(MO_m)_{n-1}] + E(MO_m) - E[(MO_m)_n] \tag{13}$$

and is the energy released for the stepwise formation of larger TMO cluster. and The DCE is the enthalpic driving force for cluster growth. The calculated DCEs for the group IVB metal oxides are in general larger than those for the group VIB metal oxides. For each of the two groups of metals, the calculated DCEs increase as the atomic number increases. The calculated DCEs for the group IVB metal oxides increase with increasing cluster size, whereas for the group VIB metal oxides, the calculated DCEs decrease with increasing cluster size. This is mainly due to the different structural evolution for the oxides of these two groups of metals. For the group VIB metals (Figure 1), the numbers of terminal and bridge oxygen atoms per metal atom remain the same from the dimer to the tetramer. However,

TABLE 12: Total Atomization Energies in kcal/mol at 0 K for the Ground States of $(MO_2)_n$ and $(M'O_3)_n$ (M = Ti, Zr, Hf; M′ = Cr, Mo, W; $n = 1-2$) Calculated at the B3LYP Level and Compared with Those Calculated at the CCSD(T)-DK Level or at the CCSD(T) Level with the Pseudopotential Corrections[a]

	$\Delta E_{n=D}$[b]	$\Delta E_{n=T}$[b]	$\Delta E_{n=Q}$[b]	ΔE_{CBS}[c]	$\Sigma D_{0,0K}$[d]	$\Delta(\Sigma D_{0,0K})$[e]
TiO_2	293.28	292.80	292.96	293.09	288.8	−8.9
ZrO_2	322.84	326.71	327.75	328.32	322.9	−5.6
HfO_2	318.01	321.89	322.78	323.25	312.1	−2.7
CrO_3	320.94	319.32	320.27	320.98	314.5	−18.3
MoO_3	406.48	412.09	413.66	414.55	408.5	−3.8
WO_3	458.80	465.56	466.68	467.22	452.7	−5.8
Ti_2O_4	704.55	703.35	703.40	703.47	692.6	−24.0
Zr_2O_4	770.15	777.51	779.62	780.79	768.1	−17.4
Hf_2O_4	779.32	787.14	788.80	789.65	765.5	−13.9
Cr_2O_6	734.97	732.69	734.67	736.09	721.1	−38.1
Mo_2O_6	921.57	934.16	937.36	939.08	925.4	−12.3
W_2O_6	1038.65	1053.06	1055.25	1056.24	1025.9	−19.6

[a] From Table 3. [b] Geometries from B3LYP/aVDZ-PP. [c] Extrapolated B3LYP energies with n = D, T, and Q using eq 1. [d] $\Sigma D_{0,0K} = \Delta E_{CBS} + \Delta E_{ZPE} + \Delta E_{SO}$, with ΔE_{ZPE} and ΔE_{SO} were taken from Table 3. [e] The difference between the B3LYP and the CCSD(T)-DK or CCSD(T) values.

for the group IVB metals, the number of terminal oxygen atoms per metal atom decreases from the dimer to the tetramer, whereas the number of bridge oxygen atoms per metal atom increases. As shown in Table 10, the bond energy for the terminal metal−oxygen M═O bond is substantially less than twice the bridge metal−oxygen bond by 45−75 kcal/mol. This results in generally larger DCEs for the group IVB metal oxides than those for the group VIB metal oxides, as more terminal oxygen atoms are converted into bridge oxygen atoms for the group IVB metal oxides than for the group VIB metal oxides.

DFT Total Atomizaton Energies. Table 12 presents the TAEs at 0 K calculated at the B3LYP level for the monomers and dimers and compares them to those calculated at the CCSD(T)-DK level or at the CCSD(T) level with the pseudopotential corrections. For M = Ti, we have previously shown that the TAEs calculated at the DFT level have much less basis set dependence than those calculated at the CCSD(T) level.[17d] As shown in Table 12, for the monomers, the basis set extrapolation effects calculated at the B3LYP level from aVDZ-PP to CBS are ~5 kcal/mol for M = Zr and Hf, and ~8 kcal/mol for M = Mo and W. For M = Ti and Cr, there is essentially no basis set effect from aVDZ-PP to CBS. For the dimers, the basis set extrapolation effects from aVDZ-PP to CBS are ~1 kcal/mol for M = Ti and Cr, ~10 kcal/mol for M = Zr and Hf, and ~17 kcal/mol for M = Mo and W. The basis set extrapolation effects from aVTZ-PP to CBS are much smaller, and for the monomers they are ~1.5 kcal/mol for M = Zr, Hf, Cr, W, and ~2.5 kcal/mol for M = Mo. For M = Ti, there is essentially no extrapolation effect from aVTZ-PP to CBS. Thus, the aVTZ-PP basis set at the DFT level should give reasonably converged TAEs; basis set extrapolation at the B3LYP level usually leads to TAEs that are larger by 1 to 2 kcal/mol.

For the monomers, the TAEs calculated at the B3LYP level are lower than those at the CCSD(T)-DK or CCSD(T) level by 3−4 kcal/mol for M = Hf and Mo, ~6 kcal/mol for M = Zr and W, ~9 kcal/mol for M = Ti, and ~18 kcal/mol for

TABLE 13: Absolute and Average Deviations in kcal/mol with Respect to Those Calculated at the CCSD(T)-DK Level or at the CCSD(T) Level with the Pseudopotential Corrections[a] for the Total Atomization Energies at 0 K for the Ground States of MO_2 and $M'O_3$ (M = Ti, Zr, Hf; M′ = Cr, Mo, W) Calculated with Various DFT Exchange−Correlation Functionals and the aVTZ-PP Basis Set at the B3LYP/aVDZ-PP Geometries

	$M(^3F_2)$[b]			$M(^5F_1)$[c]			$M'(^7S_3)$[d]					
	TiO_2	ZrO_2	HfO_2	TiO_2	ZrO_2	HfO_2	CrO_3	MoO_3	WO_3	av $M(^3F_2)$[b]	av $M(^5F_1)$[c]	av $M'(^7S_3)$[d]
B3LYP	−9.2	−7.2	−4.1	−17.9	−12.4	−9.7	−19.9	−6.2	−7.4	6.8	13.3	11.2
B3P86	+6.6	+6.9	+9.0	−9.3	−5.5	−4.3	−11.4	+1.9	−1.8	7.5	6.4	5.0
B3PW91	−2.7	−1.8	+0.3	−21.0	−17.0	−16.0	−29.9	−15.9	−19.7	1.6	18.0	21.8
B1B95	−10.5	−5.1	−1.3	−24.3	−14.8	−12.1	−44.7	−16.7	−16.2	5.6	17.1	25.9
B1LYP	−25.1	−19.7	−15.5	−31.4	−23.5	−19.8	−44.0	−25.2	−23.9	20.1	24.9	31.0
mPW1PW91	−12.3	−8.2	−5.2	−29.6	−23.5	−21.8	−47.9	−28.9	−30.6	8.6	25.0	35.8
B98	−8.9	−3.7	+0.0	−10.8	−2.4	+0.6	−11.5	+5.3	+2.8	4.2	4.6	6.5
B971	−5.8	−1.0	+2.5	−6.7	+1.5	+4.4	−2.9	+12.6	+9.9	3.1	4.2	8.4
B972	+0.4	+0.6	+2.6	−3.9	+2.2	+4.0	−14.7	+6.7	+5.2	1.2	3.4	8.9
PBE1PBE	−9.4	−5.8	−2.8	−25.4	−19.8	−17.9	−41.9	−22.8	−24.4	6.0	21.1	29.7
O3LYP	+4.8	+2.5	+3.2	−11.6	−9.4	−9.9	−14.5	−3.2	−10.4	3.5	10.3	9.3
TPSSh	−1.9	−1.8	+1.0	−17.1	−14.2	−12.8	−15.7	−6.4	−12.4	1.5	14.7	11.5
BMK	−53.9	−23.7	−10.0	−38.7	−11.3	+1.3	−20.5	+7.2	+5.5	29.2	17.1	11.1
SVWN5	+95.2	+77.6	+75.8	+74.7	+66.7	+64.4	+129.4	+124.1	+113.8	82.8	68.6	122.5
BLYP	+22.3	+13.8	+13.4	+10.2	+8.3	+7.5	+44.0	+37.8	+28.1	16.5	8.7	36.6
BP86	+37.2	+26.5	+25.0	+18.1	+13.9	+11.6	+51.8	+45.0	+32.4	29.6	14.5	43.1
BPW91	+32.2	+22.2	+20.5	+8.1	+4.2	+1.2	+34.7	+28.6	+15.5	25.0	4.5	26.3
BB95	+43.0	+32.1	+30.7	+22.7	+20.5	+18.2	+54.8	+53.8	+41.9	35.3	20.5	50.2
PW91	+40.5	+30.2	+28.6	+19.1	+15.2	+12.6	+50.8	+44.7	+32.5	33.1	15.6	42.7
mPWPW91	+35.9	+25.9	+24.2	+13.2	+9.3	+6.5	+42.0	+36.0	+23.4	28.7	9.7	33.8
PBE	+39.3	+28.7	+27.1	+18.4	+14.1	+11.5	+49.6	+43.7	+31.2	31.7	14.7	41.5
OLYP	+23.2	+14.7	+12.7	+3.7	+1.6	−1.7	+19.3	+19.9	+7.0	16.9	2.3	15.4
TPSS	+15.8	+10.6	+11.3	−1.4	−2.3	−2.9	+18.2	+17.8	+7.4	12.6	2.2	14.5
VSXC	+14.7	+5.5	+6.6	+7.8	+3.3	+4.0	+27.7	+16.4	+7.0	9.0	5.0	17.0
HCTH93	+26.2	+13.6	+11.1	+10.0	+7.3	+4.1	+17.5	+21.3	+8.0	16.9	7.2	15.6
HCTH147	+30.4	+16.8	+14.4	+18.9	+16.1	+13.7	+28.9	+32.7	+20.2	20.5	16.2	27.3
HCTH407	+27.9	+13.6	+10.8	+15.9	+12.3	+9.3	+18.3	+23.1	+11.3	17.4	12.5	17.6

[a] From Table 3. [b] The $^3F_2$ state of $(n-1)d^2ns^2$ configuration was used in eq 6 for the Ti, Zr, and Hf atoms. [c] The $^5F_1$ state of $(n-1)d^3ns^1$ configuration was used in eq 6 for the Ti, Zr, and Hf atoms. [d] The $^7S_3$ state of $(n-1)d^5ns^1$ configuration was used in eq 6 for the Cr, Mo, and W atoms.

M = Cr. The deviations for the dimers are more than double those for the monomers. Thus, the B3LYP functional substantially underestimates the TAEs of these compounds and its performance degrades with increasing cluster size. In our recent studies on some of these oxide clusters, we have shown that the BP86 and PW91 functionals significantly overestimate the TAEs for the monomers and dimers of M = Ti, Cr, Mo, and W.[17b,d]

Bergström et al. have studied the performance of various DFT functionals as well as the HF, MP2, and CISD methods for the calculations of the TAE of TiO_2.[66] For the B3LYP and BP86 functionals, they reported the calculated TAEs of TiO_2 as 286.9 and 334.4 kcal/mol, respectively, which are to be compared with our values of 288.5 and 335.0 kcal/mol calculated with the aVTZ-PP basis set. The B3P86 functional gives a value of 302.1 kcal/mol, which is the closest to our CCSD(T)-DK value of 297.7 kcal/mol. By calculating the TAE of TiO_2 using the first excited state state of Ti ($^5F_1$) instead of its ground state ($^3F_2$) and correcting the calculated TAE with the experimental energy difference between these two atomic states of 18.75 kcal/mol, they were able to improve the calculated TAEs for the X-α, BVWN, BP86, and BLYP functionals, although the deviations for these improved values from our CCSD(T)-DK value still range from 7 to 17 kcal/mol. Following a similar approach, we calculate the TAEs of TiO_2 at the B3LYP/aVTZ//B3LYP/aVDZ and BP86/aVTZ//BP86/aVDZ levels to be 279.8 and 316.0 kcal/mol, which are comparable to their values of 277.6 and 315.2 kcal/mol with the same procedure. For the HF, MP2, and CISD methods, their calculated TAEs cannot reveal the intrinsic errors associated with these methods due to the expected large basis extrapolation effects for these methods.

Table 13 presents the absolute and average deviations of the calculated TAEs for the monomers with the various DFT exchange−correlation functionals and the aVTZ-PP basis set from the CCSD(T)-DK or CCSD(T) values. The TAEs calculated at the DFT level are given as Supporting Information. For the group IVB metals, both the ground electronic state of $^3F_2$ with an $(n-1)d^2ns^2$ electron configuration and the first quintet excited state of $^5F_1$ with an $(n-1)d^3ns^1$ electron configuration were used in calculating the TAEs, whereas for the group VIB metals, the lowest septet electron state of $^7S_3$ with an $(n-1)d^5ns^1$ electron configuration was used, which is the ground electronic state for Cr and Mo. The calculated TAEs were corrected with the experimental atomic spin−orbit corrections and electron excitation energies for atomic electron excited states.[58]

For the group IVB metal oxides, the TAEs calculated with the hybrid functionals are in general much closer to the CCSD(T)-DK or CCSD(T) values than those with the pure functionals, if the $^3F_2$ state is used. In this case, hybrid functionals tend to underestimate the TAEs, whereas pure functionals tend to overestimate the TAEs. The LSDA functional, of course, overbinds. Among the functionals benchmarked, the B972, TPSSh, and B3PW91 functionals have average deviations within 2 kcal/mol, with the B972 functional having the best overall performance with an average deviation of 1.2 kcal/mol and a maximum deviation of ∼3 kcal/mol. For the group IVB metal oxides, if the $^5F_1$ state is used, the TAEs calculated with all of the hybrid functionals benchmarked except for B3P98 and BMK are in worse agreement with the CCSD(T)-DK or CCSD(T) values than if the $^3F_2$ state is used, whereas those calculated with all the pure functionals benchmarked are in better agreement. In this case, the OLYP, and TPSS functionals have average deviations ∼2 kcal/mol. This suggests that there are issues with the prediction of the atomic state splittings.

TABLE 14: Absolute and Average Deviations in kcal/mol with Respect to Those Calculated at the CCSD(T)-DK Level or at the CCSD(T) Level with the Pseudopotential Corrections[a] for the Normalized Clustering Energies at 0 K for the Ground States of $(MO_2)_2$ and $(M'O_3)_2$ (M = Ti, Zr, Hf; M′ = Cr, Mo, W) Calculated with Various DFT Exchange−Correlation Functionals and the aVTZ-PP Basis Set at the B3LYP/aVDZ-PP Geometries

	absolute deviations						
method	Ti_2O_4	Zr_2O_4	Hf_2O_4	Cr_2O_6	Mo_2O_6	W_2O_6	average
B3LYP	−2.9	−3.1	−4.1	−0.8	−2.4	−4.0	2.9
B3P86	−1.7	−1.5	−2.2	+1.4	−0.2	−1.7	1.4
B3PW91	−3.1	−3.1	−3.7	−0.3	−1.8	−3.2	2.5
B1B95	−2.1	−1.5	−1.9	+0.2	−0.2	−1.2	1.2
B1LYP	−2.2	−2.5	−3.4	−0.9	−1.9	−3.2	2.4
mPW1PW91	−1.6	−1.6	−2.1	+0.8	−0.3	−1.3	1.3
B98	−2.7	−2.6	−3.3	−0.6	−1.6	−3.0	2.3
B971	−2.6	−2.7	−3.4	−0.4	−1.6	−3.1	2.3
B972	−4.8	−4.5	−5.0	−2.4	−3.3	−4.3	4.1
PBE1PBE	−1.0	−1.1	−1.6	+1.5	+0.3	−0.8	1.1
O3LYP	−9.2	−9.2	−9.8	−5.9	−7.7	−9.4	8.5
TPSSh	−1.9	−1.8	−2.6	+0.9	−1.0	−2.6	1.8
BMK	+4.1	+3.8	+3.4	+4.5	+6.5	+5.1	4.6
SVWN5	+2.8	+2.8	+1.9	+9.8	+5.0	+1.4	4.0
BLYP	−6.8	−7.0	−8.8	−3.0	−6.7	−9.7	7.0
BP86	−5.5	−5.4	−6.8	−0.7	−4.4	−7.2	5.0
BPW91	−7.0	−6.8	−8.0	−2.2	−5.8	−8.4	6.4
BB95	−7.2	−6.5	−7.7	−2.1	−5.5	−8.3	6.2
PW91	−4.5	−4.5	−5.6	+0.4	−3.5	−6.2	4.1
mPWPW91	−5.9	−5.8	−6.9	−1.0	−4.8	−7.4	5.3
PBE	−5.0	−5.1	−6.3	−0.1	−4.0	−6.8	4.6
OLYP	−12.5	−12.4	−13.3	−8.1	−11.0	−13.2	11.8
TPSS	−3.3	−3.1	−4.2	+0.4	−2.5	−4.6	3.0
VSXC	+1.6	+0.0	−1.0	+3.8	−1.1	−2.9	1.7
HCTH93	−12.8	−12.2	−13.1	−8.4	−11.0	−13.0	11.8
HCTH147	−10.2	−9.5	−10.4	−5.8	−8.6	−10.8	9.2
HCTH407	−11.6	−11.2	−11.9	−7.2	−10.0	−12.0	10.7

[a] From Table 8.

For the group VIB metal oxides, the TAEs calculated with the hybrid functionals are again in general closer to the CCSD(T)-DK or CCSD(T) values than those with the pure functionals. The hybrid functionals also tend to underestimate the TAEs, whereas the pure functionals tend to overestimate them. The B3P86 functional has the best performance for these oxides with an average deviation of ∼5 kcal/mol and a maximum deviation of ∼11 kcal/mol.

DFT Normalized and Differential Clustering Energies. Table 14 presents the absolute and average deviations of the calculated NCEs for the dimers with the various DFT exchange−correlation functionals and the aVTZ-PP basis set from those calculated at the CCSD(T)-DK level or at the CCSD(T) level with the pseudopotential corrections. The NCEs calculated at the DFT level are given as Supporting Information. The NCEs calculated at the B3LYP level with the aVTZ-PP basis set are essentially converged toward the CBS limit, which is assumed to be true for the other functionals as well. Most functionals except for BMK, SVWN5, and VSXC underestimate these NCEs. The BMK and SVWN5 functionals overestimate these NCEs by 4−5 kcal/mol on average, whereas the VSXC functional overestimates three of them and underestimates the other three. This is consistent with the fact that the LSDA functional tends to overbind.

The benchmarked hybrid functionals in general outperform the pure functionals in the calculations of these NCEs. For

TABLE 15: Absolute and Average Deviations in kcal/mol with Respect to the CCSD(T)-DK or CCSD(T) Values[a] for the Normalized Clustering energies at 0 K for the Ground States of $(MO_2)_{3,4}$ and $(M'O_3)_{3,4}$ (M = Ti, Zr, Hf; M′ = Cr, Mo, W) Calculated with Selected DFT Exchange−Correlation Functionals and the aVTZ-PP Basis Set at the B3LYP/aVDZ-PP Geometries

	absolute deviations												
method	Ti_3O_6	Ti_4O_8	Zr_3O_6	Zr_4O_8	Hf_3O_6	Hf_4O_8	Cr_3O_9	Cr_4O_{12}	Mo_3O_9	Mo_4O_{12}	W_3O_9	W_4O_{12}	average
B3LYP	−5.5	−7.0	−5.7	−6.9	−7.8	−10.0	−1.4	−2.2	−2.2	−2.7	−3.5	−3.9	4.9
B3P86	−3.9	−4.8	−3.7	−4.3	−5.3	−6.8	+0.8	−0.3	−0.2	−1.1	−1.3	−2.0	2.9
B3PW91	−6.0	−7.4	−5.9	−7.0	−7.5	−9.4	−1.3	−2.6	−2.3	−3.2	−3.3	−4.1	5.0
B1B95	−3.8	−4.6	−3.1	−3.4	−4.4	−5.8	−1.5	−2.9	−1.2	−2.3	−1.9	−2.8	3.1
B1LYP	−4.5	−5.8	−4.8	−5.8	−6.8	−8.7	−1.5	−2.3	−1.5	−2.0	−2.5	−2.8	4.1
mPW1PW91	−3.7	−4.6	−3.7	−4.3	−5.1	−6.5	+0.0	−1.1	−0.5	−1.4	−1.1	−1.9	2.8
B98	−5.2	−6.7	−5.1	−6.2	−6.8	−8.7	−1.5	−2.4	−1.7	−2.4	−2.7	−3.2	4.4
B971	−5.0	−6.5	−5.1	−6.2	−6.8	−8.8	−1.2	−2.1	−1.7	−2.5	−2.9	−3.4	4.4
PBE1PBE	−2.7	−3.5	−3.0	−3.5	−4.4	−5.7	+0.8	−0.2	+0.2	−0.7	−0.6	−1.3	2.2
TPSSh	−4.1	−4.8	−3.8	−4.3	−5.7	−7.0	−0.1	−1.4	−1.7	−2.7	−3.0	−3.9	3.6
TPSS	−6.1	−7.2	−5.9	−6.9	−8.1	−10.0	−0.6	−2.0	−3.5	−4.7	−5.4	−6.5	5.6
VSXC	−3.1	−4.3	−0.8	−1.8	−1.1	−0.9	+5.8	+4.4	−1.2	−3.4	−2.8	−4.8	2.9

[a] CCSD(T)-DK/aVTZ-DK values from Table 8 (CCSD(T)/aVTZ-PP for Hf_3O_6, Hf_4O_8, and W_4O_{12}).

example, the PBE functional has an average deviation of 4.6 kcal/mol, whereas PBE1PBE has an average deviation of 1.1 kcal/mol. Among the hybrid functionals benchmarked, the PBE1PBE, B1B95, mPW1PW91, B3P86, and TPSSh functionals have average deviations of <2 kcal/mol. The PBE1PBE functional has the best performance with an average deviation of 1.1 kcal/mol and a maximum deviation of 1.6 kcal/mol. The popular B3LYP functional has an average deviation of 2.9 kcal/mol and a maximum deviation of 4.1 kcal/mol. Among the pure functionals benchmarked, only the VSXC functional has an average deviation of <2 kcal/mol with a maximum deviation of <4 kcal/mol. Some of the popular pure functionals such as BLYP, BP86, and BPW91 have average deviations of 5−7 kcal/mol. The SVWN5, PW91, and PBE functionals often employed in solid state calculations have average deviations of 4 to 5 kcal/mol.

To test the applicability of the above conclusions drawn by benchmarking the NCEs of the dimers, we also benchmarked those for the trimers and tetramers. Table 15 presents the absolute and average deviations of the calculated NCEs for the trimers and tetramers with 12 selected functionals from those calculated at the CCSD(T)-DK or CCSD(T) level. These functionals have average deviations of ≤3 kcal/mol for the NCEs of the dimers. The NCEs calculated at the DFT level, and their absolute and average deviations for additional functionals are given as Supporting Information. In addition, the calculated DCEs with the various exchange−correlation functionals and their deviations from the CCSD(T)-DK or CCSD(T) results are also given as Supporting Information. For calculating the NCEs, the PBE1PBE, mPW1PW91, B3P86, VSXC, and B1B95 functionals have average deviations of ≤3 kcal/mol, with the PBE1PBE functional has the least average deviation of 2.2 kcal/mol. The maximum deviation for the PBE1PBE functional is ∼6 kcal/mol. The VSXC functional has an average deviation of 2.8 kcal/mol with a similar maximum deviation. For all these functionals, the average deviations in the calculated NCEs increase with the cluster size, indicating the degradation of their performance. For example, the average deviation for the PBE1PBE functional increases from 1.1 kcal/mol for the dimers, to 1.9 kcal/mol for the trimers, and to 2.5 kcal/mol for the tetramers. Furthermore, the performance degradation for the DFT method in the calculated NCEs is actually much worse when they are used for calculating the heats of formation for the larger clusters from the monomer due to the multiplicative factor in eq 11. For example, when the NCEs calculated at the PBE1PBE level with eq 11 are used, the average errors in the calculated heats of formation due to the errors in the calculated NCEs are ∼2 kcal/mol for the dimers, ∼6 kcal/mol for the trimers, and ∼10 kcal/mol for the tetramers. Thus the performance degradation is faster than linear.

The PBE1PBE, BMK, SVWN5, and VSXC functionals predict DCEs with average deviations of ≤5 kcal/mol, and the PBE1PBE functional has the lowest average deviation of 4.5 kcal/mol. The maximum deviation for the PBE1PBE functional is ∼10 kcal/mol. The large average deviations for the calculated DCEs are due to the performance degradation for these DFT functionals.

Conclusions

The calculations described above provide for the first time reliable values for the heats of formation of transition metal oxide clusters. These values can be used to better understand the energetic properties of these catalytically active species and provide a set of benchmarks previously unavailable for testing lower level methods. The approach to the prediction of thermodynamic properties for transition metal compounds that we describe on the basis of CCSD(T)/CBS extrapolations with additional corrections is computationally expensive but is general as long as there is not a substantial amount of multireference character in the starting wave function. We expanded on our efficient and accurate approach for the prediction of the thermodynamic properties of transition metal complexes using normalized clustering energies. This approach is based on our observation that the basis set dependence of the total atomization energy and thus the derived heat of formation is much larger than the dependence of the normalized clustering energy on the basis set at the CCSD(T) level. With this approach, we have provided accurate heats of formation for the group IVB and VIB TMO clusters up to the tetramers. The approach which combines accurate heats of formation of monomers with NCEs provides a general technique for the estimation of the thermodynamics of transition metal oxide nanoclusters and holds the potential for general applicability for other transition metal-based nanoclusters. Comparison with the available experimental data indicates that our approach is capable of providing very accurate heats of formation for these clusters, although more accurate experimental heats of formation of the atoms and the clusters will allow for better assessment of our results. All of the clusters discussed above are stoichiometric with the metal atoms in the highest formal oxidation state (formal d^0 electron configuration) because these are the core types of structures observed experimentally on surfaces for catalytically active WO_3 clusters[67] and in photoelectron studies of metal oxides.[18,68] These types of structures as discussed previously[17] provide the basic frameworks for building larger metal oxides including the polymetalloxallates. However, our approach is generally applicable to other types of TMO clusters, for example those in different oxidation states or with nonstoichiometric numbers of oxygen atoms.

The calculations enabled the prediction of average M—O and M═O bond dissociation energies (BDEs). The estimated average M═O BDE follows the order Cr < Mo < Ti < W < Hf < Zr. The M═O bond energy for the same row is larger for the group IVB metal oxides than the group VIB metal oxides even though the latter nominally have a higher oxidation state of +6 as compared to +4. The M═O BDE increases with the atomic number for the group VIB metals but for the group IVB metals, the BDE increases from Ti to Zr and decreases from Zr to Hf. The average M═O BDE follows the order of Cr < Mo < Ti < W < Hf < Zr. The M═O bond energy for the same row is larger for the group IVB metal oxides than the group VIB metal oxides even though the latter nominally have a higher oxidation state of +6 as compared to +4. The M═O BDE increases with the atomic number for the group VIB metals but for the group IVB metals, the BDE increases from Ti to Zr and decreases from Zr to Hf. The average M—O BDE is surprisingly strong and is only less than that of M═O by ~30 kcal/mol for M = Cr and by 40−50 kcal/mol for the other metals.

The DCEs for the group IVB metal oxides increase with increasing cluster size, whereas the DCEs decrease for the group VIB metal oxides with increasing cluster size. The trends in BDEs together with the number of terminal and bridge M—O bonds can be used to explain the trends in the DCEs. The number of terminal and bridge oxygen atoms per metal atom remain the same from the dimer to the tetramer for the group VIB metals but for the group IVB metals, the number of terminal oxygen atoms per metal atom decreases from the dimer to the tetramer, and the number of bridge oxygen atoms per metal atom increases. The fact that the M═O BDEs are less than twice the M—O BDES results in larger DCEs for the group IVB metal oxides, which increase with increasing cluster size as more terminal oxygen atoms are converted into bridge oxygen atoms.

We have also benchmarked a large number of popular density functional theory methods in the calculations of the total atomization energies and normalized cluster energies. The hybrid functionals in general outperform the pure functionals in calculating both properties, although the accuracy of the calculated total atomization energies shows strong dependence on the choice of the atomic electronic state. The DFT functionals are shown to have serious performance degradation behavior with the increasing cluster size.

Acknowledgment. This work was supported by the Chemical Sciences, Geosciences and Biosciences Division, Office of Basic Energy Sciences, U.S. Department of Energy (DOE) under grant no. DE-FG02-03ER15481 (catalysis center program). D.A.D. also thanks the Robert Ramsay Chair Fund of The University of Alabama for support. J.M.H. thanks the Computer Based Honors Program of The University of Alabama for a scholarship. Part of this work was performed at the W. R. Wiley Environmental Molecular Sciences Laboratory, a national scientific user facility sponsored by DOE's Office of Biological and Environmental Research and located at Pacific Northwest National Laboratory, operated for the DOE by Battelle. We thank Prof. H. Stoll, Dr. D. Figgen, and Prof. M. Dolg for prepublication access to their 3d and 5d pseudopotential parameters.

Supporting Information Available: Metal−oxygen bond lengths and bond angles calculated at various levels of theory. Total atomization energies, normalized clustering energies, heats of formations, estimated metal−oxygen bond energies calculated at the CCSD(T) level with the RECP basis sets. Differences in the extrapolated B3LYP energies and calculated total atomization energies at 0 K using the exponential and mixed Gaussian/exponential formulas. Total atomization energies and normalized and differential clustering energies calculated at the DFT level with various exchange−correlation functionals and their deviations from the CCSD(T) or CCSD(T)-DK results. Energies calculated at the various levels of theory. Cartesian coordinates in Angstroms calculated at the various levels of theory. This material is available free of charge via the Internet at http://pubs.acs.org.

References and Notes

(1) Rao, C. N. R.; Raveau, B. *Transition Metal Oxides*; VCH Publishers Inc.: New York, 1995.

(2) (a) Hodnett, B. K.; Janssen, F. J. J. G.; Niemantsverdriet, J. W.; Ponec, V.; van Santen, R. A.; van Veen, J. A. R. In *Catalysis: An Integrated Approach*, 2nd ed.; van Santen, R. A., van Leeuwen, P. W. N. M., Moulijn, J. A., Averill, B. A., Eds.; Elsevier Science B. V.: Amsterdam, The Netherlands, 1999. (b) Chorkendorff, I.; Niemantsverdriet, J. W. *Concepts of Mordern Catalysis and Kinetics*, 2nd ed.; Wiley-VCH: Darmstadt, Germany, 2007.

(3) Pârvulescu, V. I.; Marcu, V. In *Surface and Nanomolecular Catalysis*, Richards, R., Ed.; CRC Press: Boca Roton, FL, 2006.

(4) (a) Pope, M. T., Müller, A., Eds. *Polyoxometalates: from Platonic Solids to Retro-viral Activity*; Kluwer Academic Publishers: Dodrecht, The Netherlands, 1994. (b) Hill, C. L. A special issue on polyoxometalates in catalysis. *J. Mol. Catalysis A: Chem* **1996**, *114*, 1–371. (c) Hill, C. L. A special issue on polyoxometalates. *Chem. Rev.* **1998**, *98*, 1–390.

(5) (a) Pople, J. A.; Head-Gordon, M.; Fox, D. J.; Raghavachari, K.; Curtiss, L. A. *J. Chem. Phys.* **1989**, *90*, 5622. (b) Curtiss, L. A.; Raghavachari, K.; Trucks, G. W.; Pople, J. A. *J. Chem. Phys.* **1991**, *94*, 7221. (c) Curtiss, L. A.; Raghavachari, K.; Redfern, P. C.; Rassolov, V.; Pople, J. A. *J. Chem. Phys.* **1998**, *109*, 7764. (d) Curtiss, L. A.; Redfern, P. C.; Raghavachari, K. *J. Chem. Phys.* **2007**, *126*, 84108.

(6) (a) Martin, J. M. L.; de Oliveira, G. *J. Chem. Phys.* **1999**, *111*, 1843. (b) Boese, A. D.; Oren, M.; Atasoylu, O.; Martin, J. M. L.; Kallay, M.; Gauss, J. *J. Chem. Phys.* **2004**, *120*, 4129. (c) Karton, A.; Rabinovich, E.; Martin, J. M. L.; Ruscic, B. *J. Chem. Phys.* **2006**, *125*, 144108.

(7) Wood, G. P. F.; Radom, L.; Petersson, G. A.; Barnes, E. C.; Frisch, M. J.; Montgomery, J. A., Jr. *J. Chem. Phys.* **2006**, *125*, 94106, and references therein.

(8) (a) Peterson, K. A.; Xantheas, S. S.; Dixon, D. A.; Dunning, T. H., Jr. *J. Phys. Chem. A.* **1998**, *102*, 2449. (b) Feller, D.; Peterson, K. A. *J. Chem. Phys.* **1998**, *108*, 154. (c) Dixon, D. A.; Feller, D. *J. Phys. Chem. A* **1998**, *102*, 8209. (d) Feller, D.; Peterson, K. A. *J. Chem. Phys.* **1999**, *110*, 8384. (e) Feller, D.; Dixon, D. A. *J. Phys. Chem. A* **1999**, *103*, 6413. (f) Feller, D. *J. Chem. Phys.* **1999**, *111*, 4373. (g) Feller, D.; Dixon, D. A. *J. Phys. Chem. A* **2000**, *104*, 3048. (h) Feller, D.; Sordo, J. A. *J. Chem. Phys.* **2000**, *113*, 485. (i) Feller, D.; Dixon, D. A. *J. Chem. Phys.* **2001**, *115*, 3484. (j) Dixon, D. A.; Feller, D.; Sandrone, G. *J. Phys. Chem. A* **1999**, *103*, 4744. (k) Ruscic, B.; Wagner, A. F.; Harding, L. B.; Asher, R. L.; Feller, D.; Dixon, D. A.; Peterson, K. A.; Song, Y.; Qian, X.; Ng, C.; Liu, J.; Chen, W.; Schwenke, D. W. *J. Phys. Chem. A* **2002**, *106*, 2727. (l) Feller, D.; Dixon, D. A.; Peterson, K. A. *J. Phys. Chem. A* **1998**, *102*, 7053. (m) Dixon, D. A.; Feller, D.; Peterson, K. A. *J. Chem. Phys.* **2001**, *115*, 2576. (n) Dixon, D. A.; Gutowski, M. *J. Phys. Chem. A* **2005**, *109*, 5129. (o) Grant, D.; Dixon, D. A. *J. Phys. Chem. A* **2005**, *109*, 10138. (p) Matus, M. H.; Anderson, K. D.; Camaioni, D. M.; Autrey, S. T.; Dixon, D. A. *J. Phys. Chem. A* **2007**, *111*, 4411. (q) Pollack, L.; Windus, T. L.; de Jong, W. A.; Dixon, D. A. *J. Phys. Chem. A* **2005**, *109*, 6934.

(9) Tajti, A.; Szalay, G.; Császár, P. G.; Kállay, M.; Gauss, J.; Valeev, E. F.; Flowers, B. A.; Vázquez, J.; Stanton, J. F. *J. Chem. Phys.* **2004**, *121*, 11599.

(10) Curtiss, L. A.; Redfern, P. C.; Raghavachari, K. *J. Chem. Phys.* **2005**, *123*, 124107.

(11) (a) DeYonker, N. J.; Cundari, T. R.; Wilson, A. K. *J. Chem. Phys.* **2006**, *124*, 114104. (b) DeYonker, N. J.; Cundari, T. R.; Wilson, A. K.; Sood, C. A.; Magers, D. H. *THEOCHEM* **2006**, *775*, 77. (c) DeYonker, N. J.; Grimes, T.; Yockel, S.; Dinescu, A.; Mintz, B.; Cundari, T. R.; Wilson, A. K. *J. Chem. Phys.* **2006**, *125*, 104111. (d) Ho, D. S.; DeYonker, N. J.; Wilson, A. K.; Cundari, T. R. *J. Phys. Chem. A* **2006**, *110*, 9767.

(12) DeYonker, N. J.; Peterson, K. A.; Steyl, G.; Wilson, A. K.; Cundari, T. R. *J. Phys. Chem. A* **2007**, *111*, 11269.

(13) (a) Purvis, G. D., III; Bartlett, R. J. *J. Chem. Phys.* **1982**, *76*, 1910. (b) Raghavachari, K.; Trucks, G. W.; Pople, J. A.; Head-Gordon, M. *Chem. Phys. Lett.* **1989**, *157*, 479. (c) Watts, J. D.; Gauss, J.; Bartlett, R. J. *J. Chem. Phys.* **1993**, *98*, 8718. (d) Bartlett, R. J.; Musial, M. *Rev. Mod. Phys.* **2007**, *79*, 291.

(14) (a) Dunning, T. H., Jr. *J. Chem. Phys.* **1989**, *90*, 1007. (b) Kendall, R. A.; Dunning, T. H., Jr.; Harrison, R. J. *J. Chem. Phys.* **1992**, *96*, 6796. (c) Woon, D. E.; Dunning, T. H., Jr. *J. Chem. Phys.* **1993**, *98*, 1358. (d) Dunning, T. H., Jr. *J. Phys. Chem. A* **2000**, *104*, 9062.

(15) (a) Peterson, K. A. *J. Chem. Phys.* **2003**, *119*, 11099. (b) Peterson, K. A.; Figgen, D.; Goll, E.; Stoll, H.; Dolg, M. *J. Chem. Phys.* **2003**, *119*, 11113. (c) Peterson, K. A.; Puzzarini, C. *Theor. Chem. Acc.* **2005**, *114*, 283. (d) Peterson, K. A.; Figgen, D.; Dolg, M.; Stoll, H. *J. Chem. Phys.* **2007**, *126*, 124101 (unpublished basis sets for the first and third row transition elements). (e) Peterson, K. A. In *Annual Reports in Computational Chemistry*; Spellmeyer, D. C., Wheeler, R. A., Eds.; Elsevier, B. V.: Amsterdam, The Netherlands, 2007; Vol. 3.

(16) Parr, R. G.; Yang, W. *Density-Functional Theory of Atoms and Molecules*; Oxford University Press: New York, 1989.

(17) (a) Li, S.; Dixon, D. A. *J. Phys. Chem. A* **2006**, *110*, 6231. (b) Li, S.; Dixon, D. A. *J. Phys. Chem. A* **2007**, *111*, 11908. (c) Li, S.; Dixon, D. A. *J. Phys. Chem. A* **2007**, *111*, 11093. (d) Li, S.; Dixon, D. A. *J. Phys. Chem. A* **2008**, *112*, 6646.

(18) Zhai, H.-J.; Li, S.; Dixon, D. A.; Wang, L.-S. *J. Am. Chem. Soc.* **2008**, *130*, 5167.

(19) Becke, A. D. *Phys. Rev. A* **1988**, *38*, 3098.

(20) Perdew, J. P. *Phys. Rev. B* **1986**, *33*, 8822.

(21) Burke, K.; Perdew, J. P., Wang, Y. In *Electronic Density Functional Thoery: Recent Progress and New Directions*; Dobson, J. F., Vignale, G., Das, M. P., Eds.; Plenum: New York, 1998.

(22) Perdew, J. P.; Wang, Y. *Phys. Rev. B* **1991**, *45*, 13244.

(23) Schultz, N. E.; Zhao, Y.; Truhlar, D. G. *J. Phys. Chem. A* **2005**, *109*, 4388.

(24) Zhao, Y.; Truhlar, D. G. *J. Chem. Phys.* **2006**, *124*, 224105.

(25) Furche, F.; Perdew, J. P. *J. Chem. Phys.* **2006**, *124*, 044103.

(26) Li, S.; Peterson, K. A.; Dixon, D. A. *J. Chem. Phys.* **2008**, *128*, 154301.

(27) Hehre, W. J.; Radom, L.; Schleyer, P. v. R.; Pople, J. A. *Ab Initio Molecular Orbtial Theory*; Wiley-Interscience: New York, 1986.

(28) Becke, A. D. *J. Chem. Phys.* **1993**, *98*, 5648.

(29) Lee, C.; Yang, W.; Parr, R. G. *Phys. Rev. B* **1988**, *37*, 785.

(30) Slater, J. C. *Quantum Theory of Molecules and Solids*; McGraw-Hill: New York, 1974; Vol. 4.

(31) Vosko, S. H.; Wilk, L.; Nusair, M. *Can. J. Phys* **1980**, *58*, 1200.

(32) Becke, A. D. *J. Chem. Phys.* **1996**, *104*, 1040.

(33) Adamo, C.; Barone, V. *J. Chem. Phys.* **1998**, *108*, 664.

(34) Perdew, J. P.; Burke, K.; Ernzerhof, M. *Phys. Rev. Lett.* **1996**, *77*, 3865.

(35) Perdew, J. P.; Burke, K.; Ernzerhof, M. *Phys. Rev. Lett.* **1997**, *78*, 1396.

(36) Handy, N. C.; Cohen, A. J. *Mol. Phys.* **2001**, *99*, 403.

(37) Tao, J. M.; Perdew, J. P.; Staroverov, V. N.; Scuseria, G. E. *Phys. Rev. Lett.* **2003**, *91*, 146401.

(38) Cohen, A. J.; Handy, N. C. *Mol. Phys.* **2001**, *99*, 607.

(39) (a) Bohmann, J. A.; Weinhold, F.; Farrar, T. C. *J. Chem. Phys.* **1997**, *107*, 1173. (b) Ruud, K.; Helgaker, T.; Bour, P. *J. Phys. Chem. A* **2002**, *106*, 7448. (c) Helgaker, T.; Ruud, K.; Bak, K. L.; Jorgensen, P.; Olsen, J. *Faraday Discuss.* **1994**, *99*, 165.

(40) Adamo, C.; Barone, V. *Chem. Phys. Lett.* **1997**, *274*, 242.

(41) Schmider, H. L.; Becke, A. D. *J. Chem. Phys.* **1998**, *108*, 9624.

(42) Hamprecht, F. A.; Cohen, A. J.; Tozer, D. J.; Handy, N. C. *J. Chem. Phys.* **1998**, *109*, 6264.

(43) Wilson, P. J.; Bradley, T. J.; Tozer, D. J. *J. Chem. Phys.* **2001**, *115*, 9233.

(44) Van Voorhis, T.; Scuseria, G. E. *J. Chem. Phys.* **1998**, *109*, 400.

(45) Boese, A. D.; Martin, J. M. L. *J. Chem. Phys.* **2004**, *121*, 3405.

(46) Peterson, K. A.; Woon, D. E.; Dunning, T. H., Jr. *J. Chem. Phys.* **1994**, *100*, 7410.

(47) Williams, T. G.; DeYonker, N. J.; Wilson, A. K. *J. Chem. Phys.* **2008**, *128*, 044101.

(48) Feller, D. *J. Chem. Phys.* **1992**, *96*, 6104; **1993**, *98*, 7059.

(49) Woon, D. E.; Dunning, T. H., Jr. *J. Chem. Phys.* **1995**, *103*, 4572.

(50) Peterson, K. A.; Dunning, T. H., Jr. *J. Chem. Phys.* **2002**, *117*, 10548.

(51) Feller, D.; Peterson, K. A.; de Jong, W. A.; Dixon, D. A. *J. Chem. Phys.* **2003**, *118*, 3510.

(52) De Jong, W. A.; Harrison, R. J.; Dixon, D. A. *J. Chem. Phys.* **2001**, *114*, 48.

(53) (a) Balabanov, N. B.; Peterson, K. A. *J. Chem. Phys.* **2005**, *123*, 64107. (b) Balabanov, N. B.; Peterson, K. A. *J. Chem. Phys.* **2006**, *125*, 074110.

(54) Frisch, M. J.; Trucks, G. W.; Schlegel, H. B.; Scuseria, G. E.; Robb, M. A.; Cheeseman, J. R.; Montgomery, J. A., Jr.; Vreven, T.; Kudin, K. N.; Burant, J. C.; Millam, J. M.; Iyengar, S. S.; Tomasi, J.; Barone, V.; Mennucci, B.; Cossi, M.; Scalmani, G.; Rega, N.; Petersson, G. A.; Nakatsuji, H.; Hada, M.; Ehara, M.; Toyota, K.; Fukuda, R.; Hasegawa, J.; Ishida, M.; Nakajima, T.; Honda, Y.; Kitao, O.; Nakai, H.; Klene, M.; Li, X.; Knox, J. E.; Hratchian, H. P.; Cross, J. B.; Bakken, V.; Adamo, C.; Jaramillo, J.; Gomperts, R.; Stratmann, R. E.; Yazyev, O.; Austin, A. J.; Cammi, R.; Pomelli, C.; Ochterski, J. W.; Ayala, P. Y.; Morokuma, K.; Voth, G. A.; Salvador, P.; Dannenberg, J. J.; Zakrzewski, V. G.; Dapprich, S.; Daniels, A. D.; Strain, M. C.; Farkas, O.; Malick, D. K.; Rabuck, A. D.; Raghavachari, K.; Foresman, J. B.; Ortiz, J. V.; Cui, Q.; Baboul, A. G.; Clifford, S.; Cioslowski, J.; Stefanov, B. B.; Liu, G.; Liashenko, A.; Piskorz, P.; Komaromi, I.; Martin, R. L.; Fox, D. J.; Keith, T.; Al-Laham, M. A.; Peng, C. Y.; Nanayakkara, A.; Challacombe, M.; Gill, P. M. W.; Johnson, B.; Chen, W.; Wong, M. W.; Gonzalez, C.; Pople, J. A. *Gaussian 03*, revision E.01; Gaussian, Inc.: Wallingford, CT, 2004.

(55) (a) Dunlap, B. I. *J. Chem. Phys.* **1983**, *78*, 3140. (b) Dunlap, B. I. *J. Mol. Struct. (THEOCHEM)* **2000**, *529*, 37.

(56) Werner, H.-J.; Knowles, P. J.; Lindh, R.; Manby, F. R.; Schütz, M.; Celani, P.; Korona, T.; Rauhut, G.; Amos, R. D.; Bernhardsson, A.; Berning, A.; Cooper, D. L.; Deegan, M. J. O.; Dobbyn, A. J.; Eckert, F.; Hampel C.; Hetzer, G.; Lloyd, A. W.; McNicholas, S. J.; Meyer W.; Mura, M. E.; Nicklass, A.; Palmieri, P.; Pitzer, R.; Schumann, U.; Stoll, H.; Stone, A. J.; Tarroni, R.; Thorsteinsson, T. *MOLPRO*, version 2006, a package of ab initio programs. See http://www.molpro.net.

(57) (a) Bylaska, E. J.; de Jong, W. A.; Kowalski, K.; Straatsma, T. P.; Valiev, M.; Wang, D.; Aprà, E.; Windus, T. L.; Hirata, S.; Hackler, M. T.; Zhao, Y.; Fan, P.-D.; Harrison, R. J.; Dupuis, M.; Smith, D. M. A.; Nieplocha, J.; Tipparaju, V.; Krishnan, M.; Auer, A. A.; Nooijen, M.; Brown, E.; Cisneros, G.; Fann, G. I.; Früchtl, H.; Garza, J.; Hirao, K.; Kendall, R.; Nichols, J. A.; Tsemekhman, K.; Wolinski, K.; Anchell, J.; Bernholdt, D.; Borowski, P.; Clark, T.; Clerc, D.; Dachsel, H.; Deegan, M.; Dyall, K.; Elwood, D.; Glendening, E.; Gutowski, M.; Hess, A.; Jaffe, J.; Johnson, B.; Ju, J.; Kobayashi, R.; Kutteh, R.; Lin, Z.; Littlefield, R.; Long, X.; Meng, B.; Nakajima, T.; Niu, S.; Pollack, L.; Rosing, M.; Sandrone, G.; Stave, M.; Taylor, H.; Thomas, G.; van Lenthe, J.; Wong, A.; and Zhang, Z. *NWChem, A Computational Chemistry Package for Parallel Computers* , version 5.1; Pacific Northwest National Laboratory: Richland, WA 99352−0999, 2007. (b) Kendall, R. A.; Aprà, E.; Bernholdt, D. E.; Bylaska, E. J.; Dupuis, M.; Fann, G. I.; Harrison, R. J.; Ju, J.; Nichols, J. A.; Nieplocha, J.; Straatsma, T. P.; Windus, T. L.; Wong, A. T. *Comput. Phys. Commun.* **2000**, *128*, 260.

(58) (a) Moore, C. E. *Atomic Energy Levels as Derived from the Analysis of Optical Spectra, Volume 1, H to V*; U.S. National Bureau of Standards Circular 467; U.S. Department of Commerce, National Technical Information Service, COM-72-50282: Washington, D.C., 1949. (b) Moore, C. E. *Atomic Energy Levels as Derived from the Analysis of Optical Spectra, Volume 2, Mo to La*; U.S. National Bureau of Standards Circular 467; U.S. Department of Commerce, National Technical Information Service, COM-72-50216, Washington, D.C., 1949. (c) Moore, C. E. *Atomic Energy Levels as Derived from the Analysis of Optical Spectra, Volume 3, Mo to La, Hf to Ac*; U.S. National Bureau of Standards Circular 467; U.S. Department of Commerce, National Technical Information Service, COM-72-50283: Washington, D.C., 1949. The spin−orbit corrections for the atoms are calculated as $\Sigma_J(2J + 1)\cdot E_J/\Sigma_J(2J + 1)$.

(59) (a) Chase, M. W., Jr. NIST-JANAF Thermochemical Tables, 4th ed., *J. Phys. Chem. Ref. Data* **1998**, Mono. 9, Suppl. 1. (b) Cox, J. D.; Wagman, D. D.; Medvedev, V. A. *CODATA Key Values for Thermodynamics*; Hemisphere Publishing Corp.: New York, 1989. The heat of formation for Ti is given in this reference at 298.15 K. The heat of formation of Ti at 0 K is obtained from this value with the correction from 0 to 298 K given in the JANAF table.

(60) Curtiss, L. A.; Raghavachari, K.; Redfern, P. C.; Pople, J. A. *J. Chem. Phys.* **1997**, *106*, 1063.

(61) Balducci, G.; Gigli, G.; Guido, M. *J. Chem. Phys.* **1985**, *83*, 1909.

(62) Balducci, G.; Gigli, G.; Guido, M. *J. Chem. Phys.* **1985**, *83*, 1913.

(63) Burns, R. P.; DeMaria, G.; Drowart, J.; Grimley, R. T. *J. Chem. Phys.* **1960**, *32*, 1363.

(64) Norman, J. H.; Staley, H. G. *J. Chem. Phys.* **1965**, *43*, 3804.

(65) Cotton, F. A.; Wilkinson, G.; Murillo, C. A.; Bochmann, M. *Advanced Inorganic Chemistry*, 6th ed.; Wiley: New York, 1999.

(66) Bergström, R.; Lunell, S.; Eriksson, L. A. *Int. J. Quantum Chem.* **1996**, *59*, 427.

(67) (a) Kim, J.; Bondarchuk, O.; Kay, B. D.; White, J. M.; Dohnálek, Z. *Catal. Today* **2007**, *120*, 186. (b) Kim, Y. K.; Rousseau, R.; Kay, B. D.; White, J. M.; Dohnálek, Z. *J. Am. Chem. Soc.* **2008**, *130*, 5059. (c) Bondarchuk, O.; Huang, X.; Kim, J.; Kay, B. D.; Wang, L. S.; White, J. M.; Dohnálek, Z. *Angew. Chem., Int. Ed.* **2006**, *45*, 4786.

(68) (a) Zhai, H. J.; Huang, X.; Waters, T.; Wang, X. B.; O'Hair, R. A. J.; Wedd, A. G.; Wang, L. S. *J. Phys. Chem. A* **2005**, *109*, 10512. (b) Zhai, H. J.; Wang, L. S. *J. Chem. Phys.* **2006**, *125*, 164315. (c) Wu, H.; Wang, L.-S. *J. Chem. Phys.* **1997**, *107*, 8221. (d) Zhai, H.-J.; Wang, L.-S. *J. Am. Chem. Soc.* **2007**, *129*, 3022.

JP810182A